Article

Control of PMSM Based on Switched Systems and Field-Oriented Control Strategy

Marcel Nicola [1,*]**, Claudiu-Ionel Nicola** [1,*]**, Dan Selişteanu** [2] **and Cosmin Ionete** [2]

[1] Research and Development Department, National Institute for Research, Development and Testing in Electrical Engineering—ICMET Craiova, 200746 Craiova, Romania
[2] Department of Automatic Control and Electronics, University of Craiova, 200585 Craiova, Romania
[*] Correspondence: marcel_nicola@yahoo.com or marcel_nicola@icmet.ro (M.N.); nicolaclaudiu@icmet.ro (C.-T.N.)

Abstract: Starting from the problem of studying the parametric robustness in the case of the control of a permanent magnet-synchronous motor (PMSM), although robust control systems correspond entirely to this problem, due to the complexity of the algorithms of the robust type, in this article the use of switched systems theory is proposed as a study option, given the fact that these types of systems are suitable both for the study of systems with variable structure and for systems with significant parametric variation under conditions of lower complexity of the control algorithms. The study begins by linearizing a PMSM model at a static operating point and continues with a systematic presentation of the basic elements and concepts concerning the stability of switched systems by applying these concepts to the control system of a PMSM based on the field-oriented control (FOC) strategy, which usually changes the value of its parameters during operation (stator resistance R_s, stator inductances L_d and L_q, but also combined inertia of PMSM rotor and load J). The numerical simulations performed in Simulink validate the fact that, for parametric variations of the PMSM structure, the PMSM control switched systems preserve qualitative performance in terms of its control. A series of Matlab programs are presented based on the YALMIP toolbox to obtain P_i matrices, by solving Lyapunov–Metzler type inequalities, and using dwell time to demonstrate stability, as well as the qualitative study of the performance of PMSM control switched systems by presenting in phase plane and state space analysis of the evolution of state vectors: ω PMSM rotor speed, i_q current, and i_d current.

Keywords: permanent magnet synchronous motor; field-oriented control; switched systems

1. Introduction

Simultaneously with the development of interest in PMSM, due to undeniable construction and performance advantages, PMSM control systems and their applications have been developed in areas such as robotics, CNC machines, computer peripherals, and aerospace engineering. These require both high performance of the control system and parametric robustness in the sense of performance preservation in case of significant variation of PMSM parameters [1–4].

Common control strategies for PMSM include FOC and direct torque control (DTC) [5–8]. If the DTC strategy provides acceptable performance but with a relatively simple control system, the FOC strategy provides both superior control performance and a control structure that can be implemented in low- and medium-cost embedded systems.

Different types of control systems can provide high performance, but variable costs of implementation in embedded systems have been developed and implemented in a particular manner depending on the applications and requirements of the PMSM control system. Thus, one can mention adaptive [9,10], predictive [11,12], and sliding mode control

(SMC) [13,14], as well as neuro-fuzzy [15,16] and computational intelligence-based control systems [17,18].

In terms of parametric robustness, robust control systems [19–21] have obviously been developed and implemented with excellent results, but the complexity of robust computational algorithms should not be neglected.

Switched systems are characterized by the fact that at certain moments of time, under the action of a switching signal, they can change their structure or parameter values. Thus, if the system changes its parameter values within a relatively large range, the use of switched systems theory [22–28] can be an alternative approach to the study of parametric robustness under the circumstances of a decrease in the complexity of the implemented algorithms.

This paper presents the FOC control strategy for the control of a PMSM by emphasizing very good control performance on the condition that implementation in an embedded system proves to be easy [29]. Elements of switched systems theory are also used to study parametric robustness.

Among the YALMIP toolbox facilities we can mention specialized solvers for the classes of problems to which it is applied, and a unitary explanation of the way to use the syntax. The studies from [30–33] were written especially by the YALMIP toolbox developers and were chosen as examples of problem classes regarding automatic robust convex programming and explicit model-predictive control (MPC) for linear parameter-varying (LPV) systems used for stability and optimality. With the help of the YALMIP toolbox, Lyapunov–Metzler-type inequalities can be solved, which is the way to demonstrate the stability of switched systems.

Compared to other elements of qualitative analysis for systems stability with time-varying parameters, among which we can list Kharitonov's theorem, the Nyquist stability criterion, and the Bode characteristics with other design elements of robust controllers for PMSM presented in [34], solving the Lyapunov–Metzler-type inequalities can produce information regarding system stability even under the conditions of some parametric and structural changes.

The main contributions of this paper can be summarized as follows:

- PMSM model linearization at a static operating point;
- Basic elements and concept summary of switched-systems stability;
- Application of FOC control strategy and control switched systems for the control of a PMSM under significant variation of parameters that usually change value during operation (stator resistance R_s, stator inductances L_d and L_q, but also combined inertia of PMSM rotor and load J);
- Matlab/Simulink program implementation for calculation of the control system characteristic matrices under parametric variations, calculation of the positive definite matrices P_i from Lyapunov–Metzler inequalities to demonstrate system stability;
- Matlab program implementation for calculation of the dwell time;
- Numerical simulations development for the PMSM control switched systems using a switching signal with frequency lower than the one corresponding to the dwell time;
- Qualitative study of the PMSM control system performance by presenting in phase plane and state space the evolution of state vectors: ω PMSM rotor speed, i_q current, and i_d current.

The rest of the paper is organized as follows. The PMSM mathematical model and the FOC-type strategy are presented in Section 2, and the basic concepts of the switched systems are presented in Section 3. The numerical simulations realized in Matlab/Simulink programming and numerical computing environment for the PMSM control switched systems are presented in Section 4, while the final section presents conclusions and perspectives on future approaches.

2. PMSM Mathematical Model and FOC-Type Strategy

The FOC–PMSM control strategy shown as a block diagram in Figure 1 emphasizes the two cascade control loops; inner loop for current control and outer loop for the PMSM rotor speed control.

The mathematical model of the PMSM is a nonlinear one, and is presented by the relations in the system (1) [5–8].

$$\begin{cases} \dfrac{di_d}{dt} = -\dfrac{R_s}{L_d}i_d + \dfrac{L_q}{L_d}n_p\omega i_q + \dfrac{1}{L_d}u_d \\[2mm] \dfrac{di_q}{dt} = -\dfrac{R_s}{L_q}i_q - \dfrac{L_d}{L_q}n_p\omega i_d - \dfrac{\lambda_0}{L_q}n_p\omega + \dfrac{1}{L_q}u_q \\[2mm] \dfrac{d\omega}{dt} = \dfrac{3}{2}\dfrac{n_p}{J}\left(\lambda_0 i_q + \left(L_d - L_q\right)i_d i_q\right) - \dfrac{1}{J}T_L - \dfrac{B}{J}\omega \\[2mm] \dfrac{d\theta_e}{dt} = n_p\omega \end{cases} \tag{1}$$

where u_d, u_q and i_d, i_q denote the stator voltages and stator currents of the PMSM, respectively, these relations being valid in the d–q reference frame. We have denoted the stator inductances and resistances of the PMSM in the d–q reference frame as L_d, L_q and R_d, R_q. We also denoted the stator resistance of the PMSM as R_s, the PMSM rotor speed as ω, the flux linkage as λ_0, the number of pair poles as n_p, the PMSM rotor moment inertia combined with load moment inertia as J, the load torque as T_L, and finally the viscous friction coefficient as B.
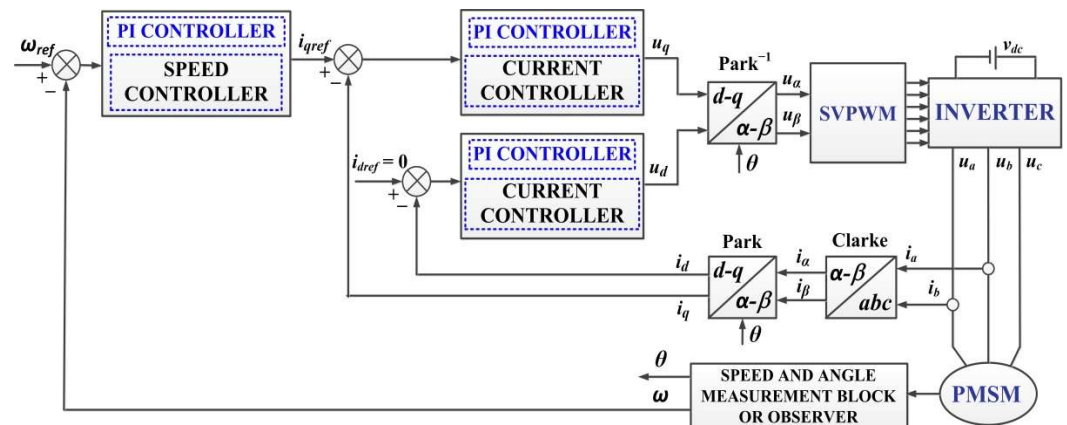

Figure 1. General block diagram for PMSM control system based on FOC-type strategy.

For $L_d = L_q$ system (1) can be written under the usual form given by the system (2).

$$\begin{bmatrix} \dot{i}_d \\ \dot{i}_q \\ \dot{\omega} \end{bmatrix} = \begin{bmatrix} -\dfrac{R_s}{L_q}i_d + n_p\omega i_q \\[2mm] -\dfrac{R_s}{L_q}i_q - n_p\omega i_d - \dfrac{\lambda_0}{L_q}n_p\omega \\[2mm] \dfrac{3}{2}\dfrac{n_p\lambda_0}{J}i_q - \dfrac{B}{J}\omega \end{bmatrix} + \begin{bmatrix} \dfrac{1}{L_q} & 0 \\[2mm] 0 & \dfrac{1}{L_q} \\[2mm] 0 & 0 \end{bmatrix}\begin{bmatrix} u_d \\ u_q \end{bmatrix} + \begin{bmatrix} 0 \\ 0 \\ -\dfrac{T_L}{J} \end{bmatrix} \tag{2}$$

The linearization of the PMSM nonlinear model are achieved around an operating point (x^*, u^*), where the states and commands are given in (3):

$$\underline{x}^* = \begin{bmatrix} i_d^* & i_q^* & \omega^* \end{bmatrix}^T ; \quad \underline{u}^* = \begin{bmatrix} u_d^* & u_q^* \mid T_L \end{bmatrix}^T \tag{3}$$

The following equilibrium relation can be written around this operating point:

$$f\left(x^*, u^*\right) = 0 \tag{4}$$

A linear system described in (5) can also be associated with the system (3):

$$\begin{cases} \dot{x}(t) = \boldsymbol{A}x(t) + \boldsymbol{B}w(t) + \boldsymbol{D}u(t) \\ \qquad y(t) = \boldsymbol{C}x(t) \end{cases} \tag{5}$$

where

$$\boldsymbol{A} = \begin{bmatrix} -\dfrac{R_s}{L_q} & n_p\omega^* & n_p i_q^* \\ n_p\omega^* & -\dfrac{R_s}{L_q} & \dfrac{-n_p\lambda_0}{L_q} \\ 0 & \dfrac{3}{2}\dfrac{n_p\lambda_0}{J} & -\dfrac{B}{J} \end{bmatrix}; \boldsymbol{B} = \begin{bmatrix} \dfrac{1}{L_q} & 0 & 0 \\ 0 & \dfrac{1}{L_q} & 0 \\ 0 & 0 & -\dfrac{1}{J} \end{bmatrix}; \boldsymbol{C} = \begin{bmatrix} 1 & 0 & 0 \\ 0 & 0 & 1 \end{bmatrix}; \boldsymbol{D} = \begin{bmatrix} 0 & 0 & 0 \\ 0 & 0 & 0 \end{bmatrix} \tag{6}$$

As a typical example of the static operating point, we can choose a state vector of the PMSM control system defined in the relation (7).

$$\begin{bmatrix} i_d^* \\ i_q^* \\ \omega^* \end{bmatrix} = \begin{bmatrix} 0 \\ 1 \\ 1200 \end{bmatrix} \tag{7}$$

3. Switched Systems—A General Description

Hybrid systems can generally be defined as systems in which continuous and discrete actions and states dynamically interact with each other. Of these systems, those that are continuous, but influenced by discrete events and have the effect of continuously changing the described dynamics, define the switched-type systems. To be define them more accurately, the differential system [22–24]

$$\dot{x}(t) = f(x(t)) \tag{8}$$

can be considered, where $f : R^n \rightarrow R^n$ is a Lipschitz function.

System (8) can be rewritten in the following form, which characterizes a switched system:

$$\dot{x}(t) = f_{\sigma(t)}(x(t)) \tag{9}$$

where there are N smooth vector fields, $f_i, i \ldots N$, and there is also a switching signal piecewise constant $\sigma : R_+ \rightarrow [1, N]$.

For example, the equations defining the temperature pattern in a heated room can be written as [22–24]:

$$\begin{cases} \dot{\theta}(t) = -\lambda\left(\theta(t) - \theta_{ext}(t)\right), \text{if the action heater is off} \\ \dot{\theta}(t) = -\lambda\left(\theta(t) - \theta_{ext}(t)\right) + \beta, \text{if the action heater is on} \end{cases} \tag{10}$$

where θ represents the room temperature and λ and β are two quantities which characterize the heating process. Based on these, system (10) can be written as a switched system:

$$\dot{\theta}(t) = -\lambda\left(\theta(t) - \theta_{ext}(t)\right) + \beta\sigma(t), \ \sigma(t) \in \{0,1\} \tag{11}$$

For the linear case, the switched systems can be written as

$$\dot{x}(t) = A_{\sigma(t)}x(t), \ x(0) = x_0 \tag{12}$$

A necessary condition for the stability of the switching system where the switching random function $\sigma(t) = i, \forall t$ is that all matrices $A_i, i = 1, \ldots, N$ are Hurwitz.

If $\sigma(t)$ is a switching signal defined for example as in the following expression:

$$\sigma(t) = \begin{cases} 2, & t \in [0, T) \\ 1 & t \in [T, 2T) \end{cases} \tag{13}$$

where $2T$ is the period of the system, and $\Phi(t, \tau)$ is the transition matrix of the system (12) considered periodic in this example, the monodromy matrix is defined as

$$\Phi(2T, 0) = e^{A_2 T} e^{A_1 T} \tag{14}$$

According to [23] the system is asymptotically stable if the monodromy matrix has subunit eigenvalues modulus.

For the general form of the linear case, one can consider the switched systems

$$\begin{cases} \dot{x}(t) = A_{\sigma(t)} x(t) + B_{\sigma(t)} u(t) \\ y(t) = C_{\sigma(t)} x(t) + D_{\sigma(t)} u(t) \end{cases} \tag{15}$$

where the notations are the usual ones, and $A_i, i = 1, \ldots, N$, are Hurwitz matrices.

There is the matter of finding the minimum of $\gamma > 0$ for which

$$\sup_{w \in L_2(0, \infty)} \frac{\|y\|_2}{\|w\|_2} < \gamma \tag{16}$$

and γ fulfills the condition

$$\gamma \geq \max_i \{\gamma_i\} \tag{17}$$

wher: γ_i is the H_∞ norm associated with the system (A_i, B_i, C_i, D_i) defined in relation (16).

In this respect the following theorem is presented [24–26]:

Theorem 1. Given the system (15) and assuming that there is a positive definite matrix P so that the following relation is satisfied,

$$\begin{bmatrix} A_i^T P + PB_i & PB_i & C_i^T \\ B_i^T P & -\gamma^2 I & D_i^T \\ C_i & D_i & -I \end{bmatrix} < 0, \forall i \in N \tag{18}$$

then the global asymptotic stability of the switched systems (15) is ensured for the switching signal σ and in addition the following inequality is fulfilled:

$$\sup_{w \in L_2, \, w \neq 0} \int_0^\infty \left(y^T y - \gamma^2 w^T w \right) dt < 0 \tag{19}$$

Proof of Theorem 1. From Schur's lemma and from (18), the inequality $\gamma^2 I - D_i^T D_i > 0$ and the relation (20) are obtained.

$$A_i^T P + PA_i + \left(PB_i + C_i^T D_i \right) \left(\gamma^2 I - D_i^T D_i \right)^{-1} \left(PB_i + C_i^T D_i \right)^T + C_i^T C_i < 0, \forall i \tag{20}$$

Based on these, relation (21) ensures the global asymptotic stability in the case of random switching for any input w square-integrable.

$$A_i^T P + PA_i < 0 \tag{21}$$

This is equivalent to choosing a Lyapunov function $V(x) = x^T P x$ whose derivative $\dot{V} < 0$.

$$w^* = \left(\gamma^2 I - D_i^T D_i\right)^{-1}\left(P_i B_i + C_i^T D_i\right)^T x \tag{22}$$

Based on notation (22), the next relation is obtained:

$$\dot{V}(x) = x^T\left(A_\sigma^T P + P A_\sigma\right)x + 2x^T P B_\sigma w <$$
$$< -y^T y + \gamma^{-2} w^T w - \left(w - w^*\right)^T\left(\gamma^2 I - D_i^T D_i\right)\left(w - w^*\right) \tag{23}$$
$$< -y^T y + \gamma^{-2} w^T w$$

and from this, by integrating $\dot{V}$, the relation (24) is obtained, which represents the conclusion of the proof of the theorem.

$$\int_0^\infty \left(y^T y - \gamma^2 w^T w\right)dt < 0,\ \forall \sigma,\ \forall w \neq 0,\ w \in L_2 \tag{24}$$

Let us consider $\alpha_i, i = 1,\ldots,N$, a simplex, i.e., $\alpha_i \geq 0$ and $\sum_{i=1}^N \alpha_i = 1$, and using the relation (18) accordingly, by applying Schur's lemma we obtain the relation (20) in condensed form (25):

$$A_\alpha^T P + P A_\alpha + \left(PB_\alpha + C_\alpha^T D_\alpha\right)\left(\gamma^2 I - D_\alpha^T D_\alpha\right)^{-1}\left(PB_\alpha + C_\alpha^T D_\alpha\right)^T + C_\alpha^T C_\alpha < 0 \tag{25}$$

where

$$A_\alpha = \sum_{i=1}^N \alpha_i A_i, \quad B_\alpha = \sum_{i=1}^N \alpha_i B_i, \quad C_\alpha = \sum_{i=1}^N \alpha_i C_i, \quad D_\alpha = \sum_{i=1}^N \alpha_i D_i \tag{26}$$

Under these conditions, norm H_∞ of the system $\left(A_\alpha, B_\alpha, C_\alpha, D_\alpha\right)$ is less than γ for any α in the considered simplex.

The following are two examples that ensure a better understanding of what has been presented so far and of how the presentation continues.

3.1. Example 1

Let us consider a switching system described by the following subsystems defined by the matrices:

$$A_1 = \begin{bmatrix} -3 & 1 \\ 0 & -1 \end{bmatrix}, \quad A_2 = \begin{bmatrix} -2 & 1 \\ 0 & -5 \end{bmatrix} \tag{27}$$

Using the Matlab environment, the eigenvalues are calculated as follows: $eig(A_1) = \{-3, -1\}$ and $eig(A_2) = \{-2, -5\}$. The result is that A_1 and A_2 are Hurwitz matrices. By applying the relation (21), we obtain the next system:

$$\begin{cases} A_1^T P + P A_1 < 0 \\ A_2^T P + P A_2 < 0 \end{cases} \tag{28}$$

Using the Matlab environment and YALMIP toolbox, the matrix P containing the solution to the system (28) is obtained as:

$$P = \begin{bmatrix} 0.2849 & 0.0359 \\ 0.0359 & 0.1821 \end{bmatrix} \tag{29}$$

Since $eig(P) = \{0.1708, 0.2969\}$, matrix P is positive definite and ensures the global asymptotic stability of the switched systems defined by (27).

3.2. Example 2

Let us consider a switching system described by the following subsystems defined by the matrices:

$$A_1 = \begin{bmatrix} -1 & -1 \\ 1 & -1 \end{bmatrix}, \quad A_2 = \begin{bmatrix} -1 & -10 \\ 0.1 & -1 \end{bmatrix} \tag{30}$$

Using the Matlab environment, the eigenvalues are calculated as $eig(A_1) = eig(A_2) = \{-1.0000 + 1.0000i, -1.0000 - 1.0000i\}$ from which it results that A_1 and A_2 are Hurwitz matrices.

Following the above method, it is demonstrated that there is no matrix $P > 0$ which verifies the system (28). Thus, the above theorem cannot be applied and it cannot be stated that the switched system described by (30) is stable even if the two subsystems are stable. This proves once again that local stability does not imply global stability, and the conditions imposed by a system such as (28) are too restrictive. In contrast, Theorem 2, below, has more restrictive conditions but ensures the stability of the switched systems [24].

First, the term dwell time is described by the following definition [25–27]:

Definition 1. *If* $T > 0, T \in R$ *so that*

$$\inf_q \left(t_q - t_{q-1} \right) \geq T \tag{31}$$

then T is called dwell time of the switched systems.

Theorem 2. *Assume that for* $T > 0$ *there is a set of positive definite matrices* $\{P_1, \ldots, P_N\}$ *of corresponding dimensions, so as to fulfill the inequalities:*

$$A_i^T P_i + P_i A_i < 0, \quad \forall i \in \{1, \ldots, N\} \tag{32}$$

$$e^{A_i^T T} P_j e^{A_i T} - P_j < 0, \quad \forall i \neq j, \quad i, j \in \{1, \ldots, N\} \tag{33}$$

Under these conditions, the time switching control law $\sigma(t) = i \in \{1, \ldots, N\}, \quad t \in [t_k, t_{k+1})$ *where* t_k *and* t_{k+1} *are successive switching moments so that* $t_{k+1} - t_k \geq T, \forall k \in \mathbf{N}$ *ensures the global asymptotic stability of the switched system.*

Proof of Theorem 2. A draft of the demonstration consists in the fact that by choosing a Lyapunov function

$$\dot{V}(x(t)) = x(t)^T P_{\sigma(t)} x(t) \tag{34}$$

and calculating its derivative, the next relation is obtained:

$$\dot{V}(x(t)) = x(t)^T \left(A_i^T P_i + P_i A_i \right) x(t) < 0 \tag{35}$$

From this, $\alpha > 0$ and $\beta > 0$ so that

$$\|x(t)\|^2 \leq \beta e^{-\alpha(t-t_k)} V(x(t_k)), \forall t \in [t_k, t_{k+1}) \tag{36}$$

By exploiting the relation (34) the next form can be obtained:

$$\begin{aligned}
\dot{V}(x(t_{k+1})) &= x(t_{k+1})^T P_j x(t_{k+1}) = x(t_k)^T e^{A_i^T T_k} P_j e^{A_i T_k} x(t_k) \\
&< x(t_k)^T e^{A_i^T (T_k - T)} P_i e^{A_i (T_k - T)} x(t_k) \\
&< x(t_k)^T P_i x(t_k) \\
&< V(x(t_k))
\end{aligned} \tag{37}$$

This results in $\mu \in (0,1)$ so that

$$V(x(t_k)) \le \mu^k V(x_0), \forall k \in \boldsymbol{N} \tag{38}$$

From relations (36) and (38) the global asymptotic stability of the switched system is obtained. It can be pointed out that inequalities (32) and (33) are known as Lyapunov–Metzler inequalities.

A number of ways of estimating the dwell time of the switched systems are presented in [26,27], where we propose an estimate used in practical examples. An upper limit for the minimum dwell time T* is given by T* $T^* \le \max\limits_{i=1,\dots,N} \{T_i\}$, where

$$T_i = \inf_{\alpha>0, \beta>0} \left\{ \frac{\alpha}{\beta} : \left\| e^{A_i t} \right\| < e^{(\alpha - \beta t)}, \forall t \ge 0 \right\} \tag{39}$$

Evidently, by using the above theorems, the stability of a switched system can be demonstrated if the switching signal does not switch more often than the dwell time. In terms of establishing a control law of a switched system, similarly to the way the above Lyapunov functions have been chosen, corresponding control laws can be obtained for the closed loop system.

4. Numerical Simulations for PMSM Control Switched Systems

For the PMSM control in the classical structure (Figure 1), the so-called FOC control strategy, with the outer speed control loop supplying the references for the inner i_d and i_q current control loops, Figure 2 shows the implementation in Matlab/Simulink, noting that the current reference i_{dref} is set to 0 for the maximization of the electromagnetic torque T_e.

Usually, the controllers of the two inner current control loops and the controller of the outer PMSM rotor speed control loop are of PI type.
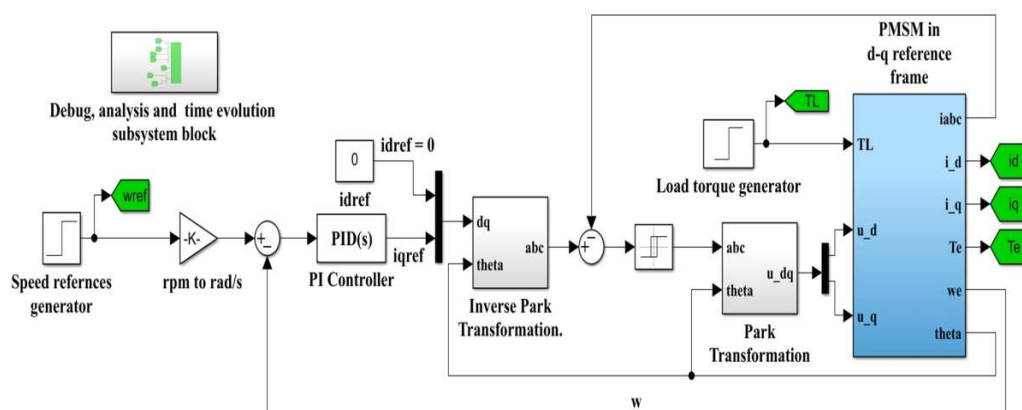

Figure 2. Simulink implementation for PMSM control system based on FOC-type strategy.

Below the numerical simulations are presented for the control system of a PMSM, with nominal parameters as given in Table 1.

Table 1. PMSM nominal parameters.

Parameter	Value	Unit
Stator resistance—R_s	2.875	Ω
Inductances on *d-q* axis—L_d , L_q	0.0085	H
Combined inertia of PMSM rotor and load—J	0.008	kg·m²
Combined viscous friction of PMSM rotor and load—B	0.01	N·m·s/rad

Flux induced by the permanent magnets of the PMSM rotor in the stator phases—λ_0	0.175	Wb
Pole pairs number—n_p	4	–

Figure 3 shows the evolution of the parameters of interest (rotor speed noted with ω, electromagnetic and load torques noted with T_e and T_L, stator currents noted with i_a, i_b, i_c, and d-q frame currents noted with i_d and i_q) of the PMSM control system based on the classic FOC control structure with PI-type controllers, following the numerical simulations by applying two-step signals for the speed reference ω_{ref} = [800, 1200] rpm and a load torque T_L of 0.5 Nm. It can be noted that the PMSM control system demonstrates good performance.
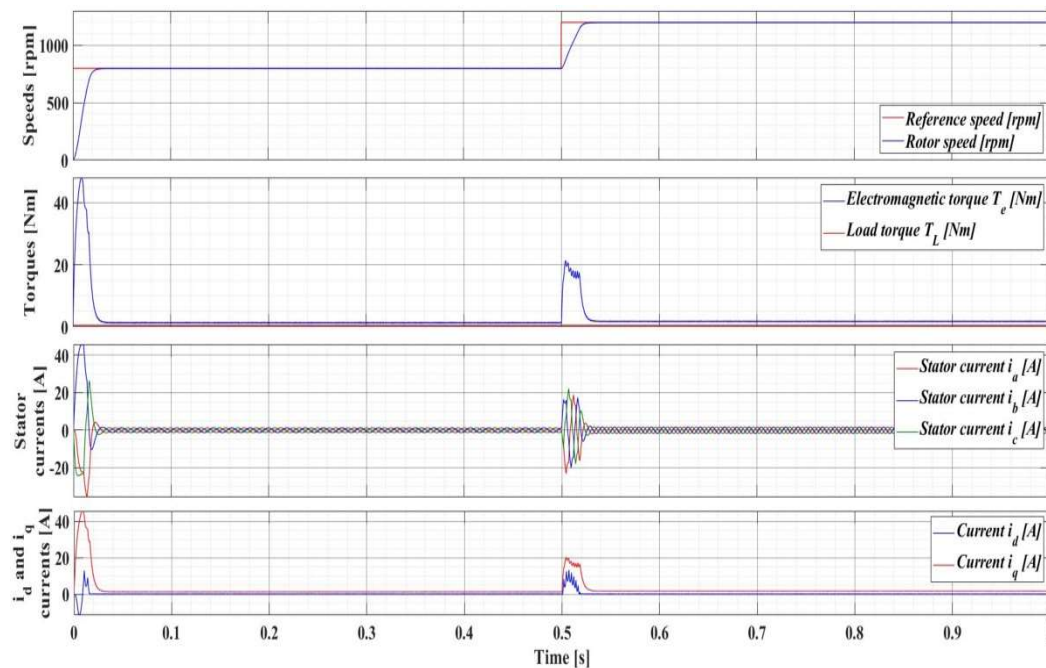
Figure 3. Time evolution parameters of the PMSM control system based on FOC-type strategy: ω_{ref} = [800, 1200] rpm and T_L = 0.5 Nm.

In addition, Figures 4–6 show the evolution of the PMSM control system states (ω PMSM rotor speed, i_q current, and i_d current) in the form of the phase plan for their corresponding combinations.

Moreover, for two successive steps of the PMSM reference speed, Figures 7 and 8 show the evolution in state plane. It can be noted that the steady-state conditions are achieved after a relatively fast transient regime and damped oscillations.
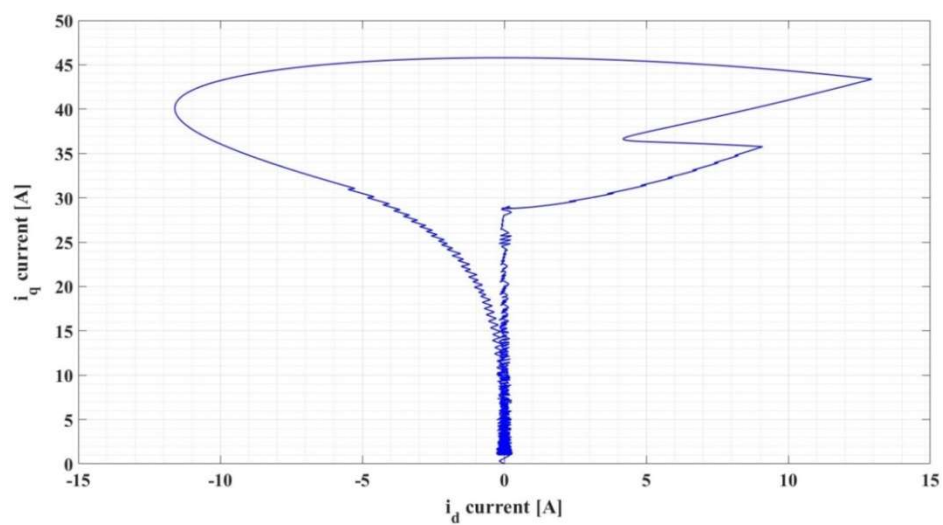
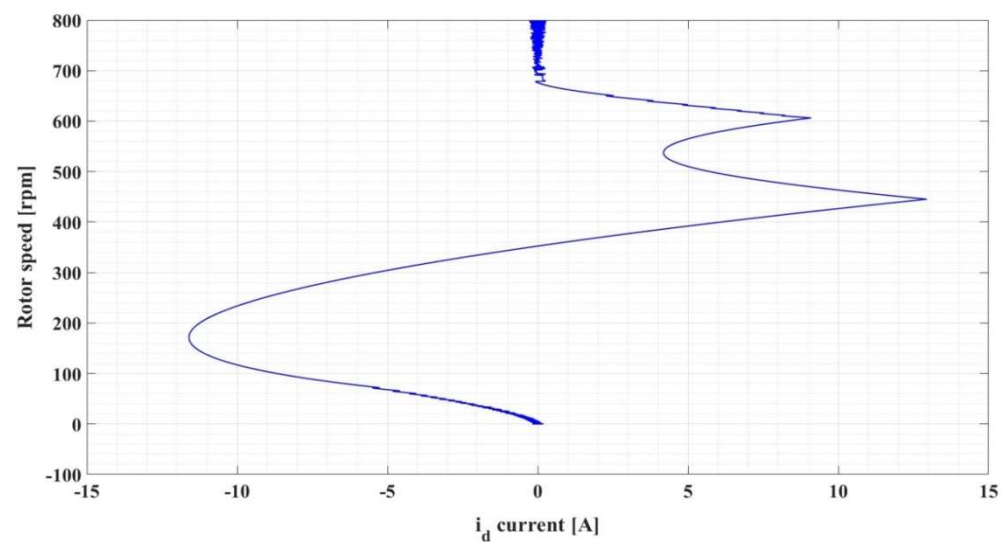**Figure 4.** Image of the phase plan: i_q current versus i_d current.

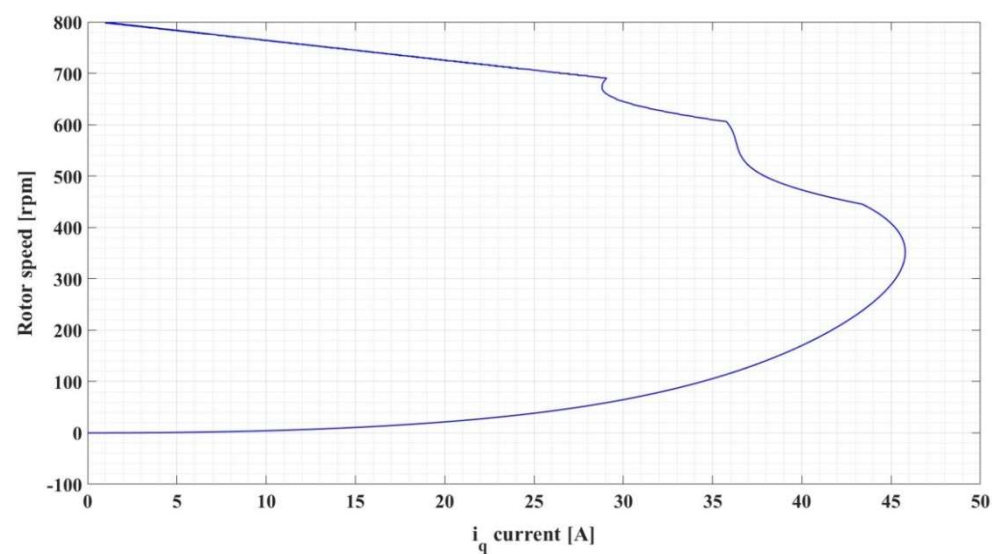**Figure 5.** Image of the phase plan: rotor speed versus i_d current.

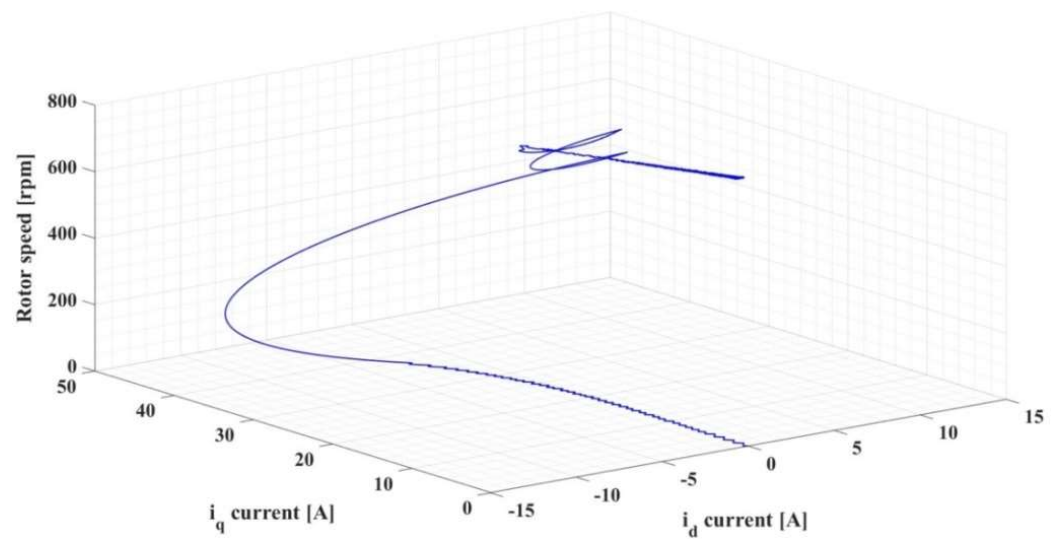**Figure 6.** Image of the phase plan: rotor speed versus i_q current.

Figure 7. Image of the state space: rotor speed versus i_q current versus i_d current (ω_{ref} = 800 rpm).
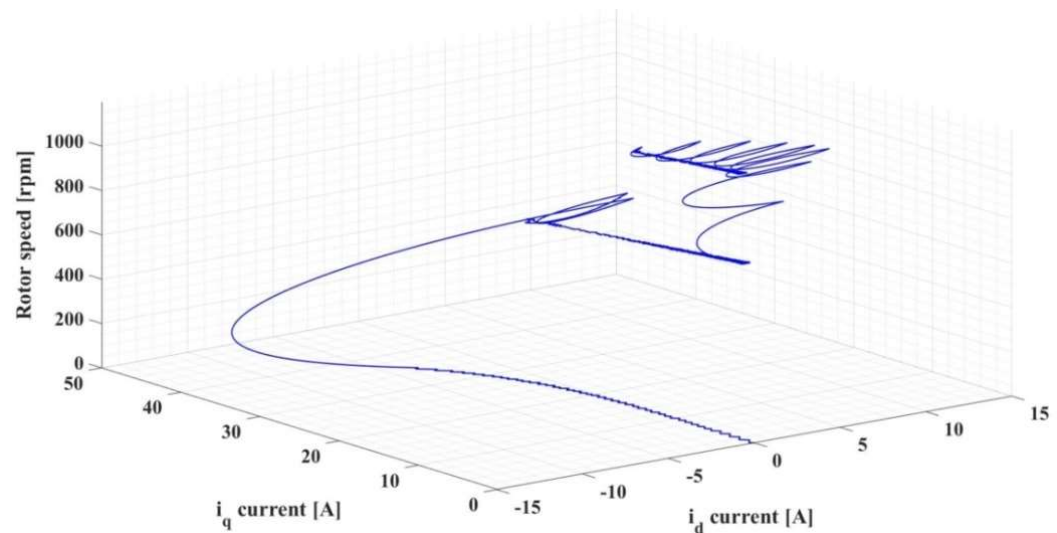

Figure 8. Image of the state space: rotor speed versus i_q current versus i_d current (ω_{ref} = [800, 1200] rpm).

In the case of the PMSM control, it can be noted that a number of its parameters may vary. These include stator resistance R_s, stator inductances L_d and L_q, but also combined inertia of PMSM rotor and load J.

Thus, using the notions described in Section 3 for switched systems, it is possible to achieve a qualitative study on the behavior of the PMSM control system in case of parametric variation.

Thus, Figure 9 shows the general block diagram for PMSM control system based on FOC-type strategy and switched systems.

The parametric structure of the PMSM is considered to change over time, and the time points at which these changes occur are correlated with an external signal called the switching signal.

Thus, Figures 10 and 11 show the Matlab/Simulink implementation for PMSM control system based on FOC-type strategy for PMSM variable structure with switching signal type 1.
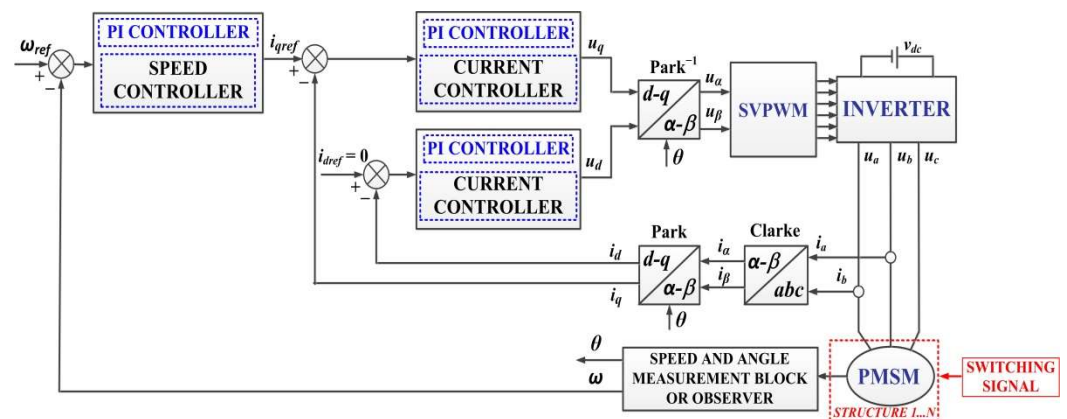
Figure 9. General block diagram for PMSM control system based on FOC-type strategy and switched systems.
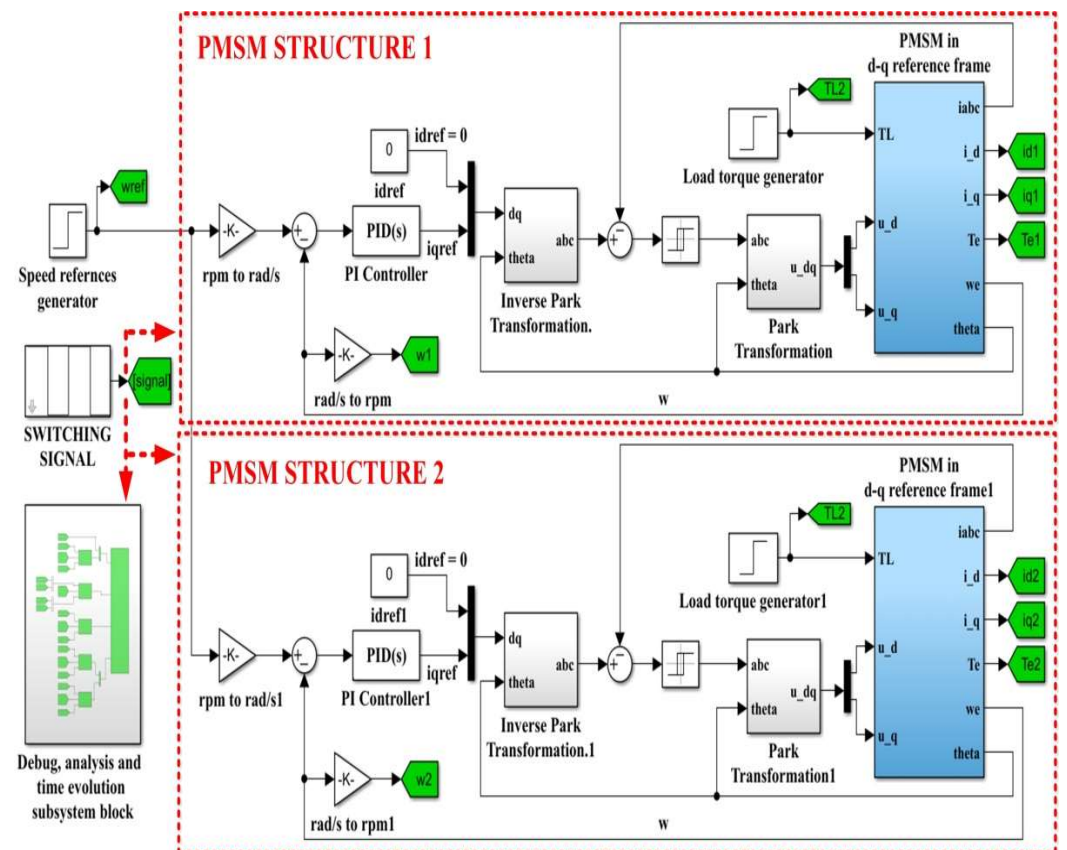

Figure 10. Simulink implementation for PMSM control system based on FOC-type strategy for PMSM variable structure with switching signal type 1.
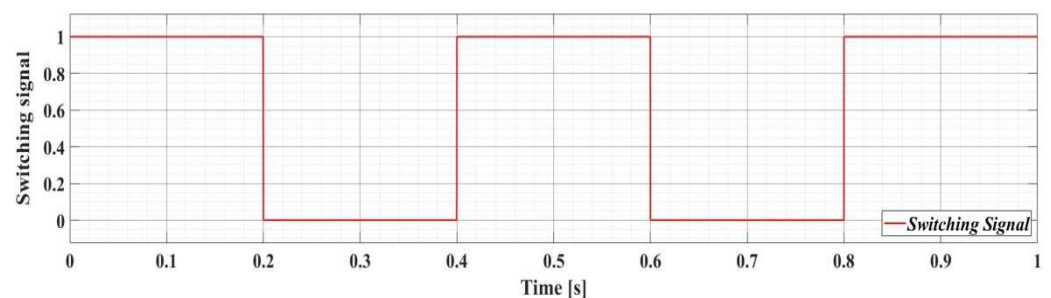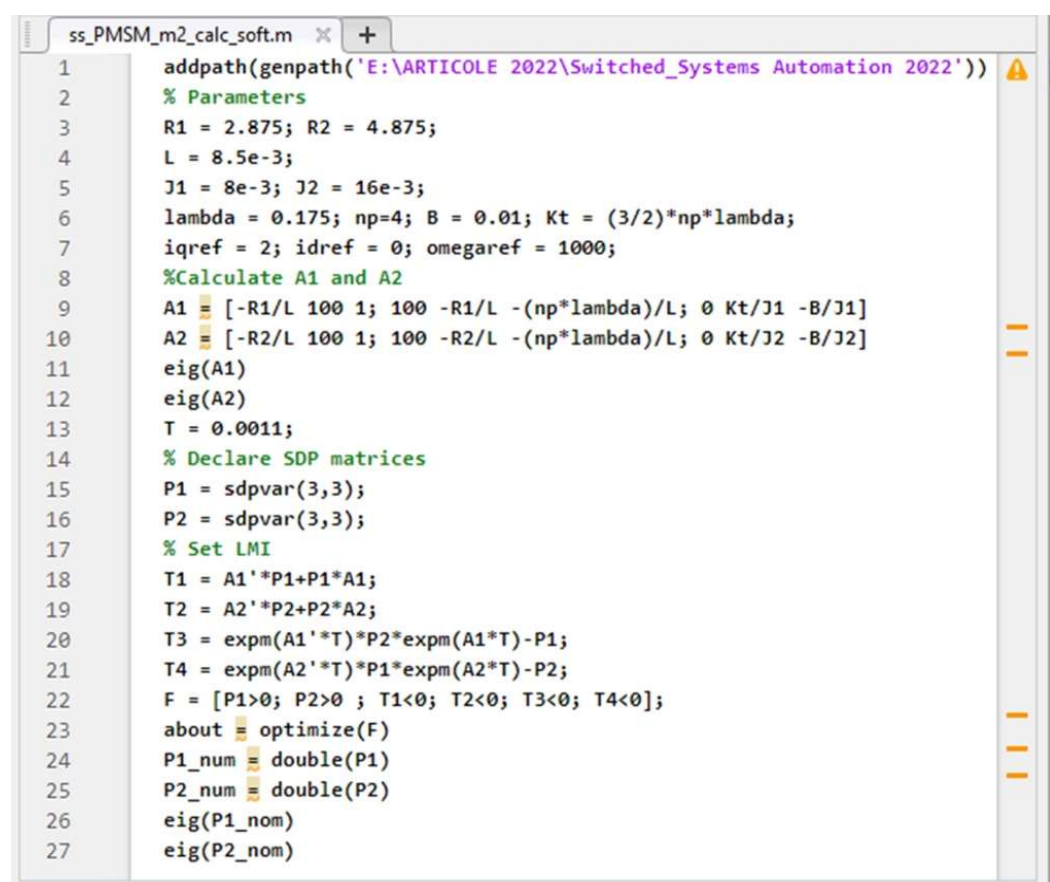

Figure 11. Switching signal type 1.

It is considered that the variation of the PMSM parameters corresponds to that shown in Table 2.

Table 2. PMSM variation parameters—variable structure 1.

Parameter	Value 1	Value 2	Unit
Stator resistance—R_s	2.875	4.875	Ω
Combined inertia of PMSM rotor and load—J	0.008	0.016	kg·m²

For the verification of Lyapunov–Metzler inequalities, Figure 12 shows the diagram of a program implemented in Matlab using the YALMIP toolbox.

```
ss_PMSM_m2_calc_soft.m  ✕   +
1       addpath(genpath('E:\ARTICOLE 2022\Switched_Systems Automation 2022'))
2       % Parameters
3       R1 = 2.875; R2 = 4.875;
4       L = 8.5e-3;
5       J1 = 8e-3; J2 = 16e-3;
6       lambda = 0.175; np=4; B = 0.01; Kt = (3/2)*np*lambda;
7       iqref = 2; idref = 0; omegaref = 1000;
8       %Calculate A1 and A2
9       A1 = [-R1/L 100 1; 100 -R1/L -(np*lambda)/L; 0 Kt/J1 -B/J1]
10      A2 = [-R2/L 100 1; 100 -R2/L -(np*lambda)/L; 0 Kt/J2 -B/J2]
11      eig(A1)
12      eig(A2)
13      T = 0.0011;
14      % Declare SDP matrices
15      P1 = sdpvar(3,3);
16      P2 = sdpvar(3,3);
17      % Set LMI
18      T1 = A1'*P1+P1*A1;
19      T2 = A2'*P2+P2*A2;
20      T3 = expm(A1'*T)*P2*expm(A1*T)-P1;
21      T4 = expm(A2'*T)*P1*expm(A2*T)-P2;
22      F = [P1>0; P2>0 ; T1<0; T2<0; T3<0; T4<0];
23      about = optimize(F)
24      P1_num = double(P1)
25      P2_num = double(P2)
26      eig(P1_nom)
27      eig(P2_nom)
```

Figure 12. Matlab program for matrices A_i and P_i determination—variable structure 1.

The matrices A_1 and A_2 are obtained similarly to the following relations (40):

$$A_1 = \begin{bmatrix} -338.2353 & 100 & 1 \\ 100 & -338.2353 & -82.3529 \\ 0 & 131.25 & -1.25 \end{bmatrix}; \quad A_2 = \begin{bmatrix} -573.5294 & 100 & 1 \\ 100 & -573.5294 & -82.3529 \\ 0 & 65.625 & -0.625 \end{bmatrix} \quad (40)$$

Using the Matlab environment, the eigenvalues are calculated as follows: $eig(A_1)$ = {−426.1689, −209.2358, −42.316}, and $eig(A_2)$ = {−669.5222 −467.6463, −10.5154}. This results in A_1 and A_2 being Hurwitz matrices.

Using the Matlab environment and YALMIP toolbox, the matrices P_1 and P_2 containing the solution to the system are obtained as follows:

$$P_1 = \begin{bmatrix} 0.0016 & 0.0013 & 0.0019 \\ 0.0013 & 0.0046 & 0.0077 \\ 0.0019 & 0.0077 & 0.0221 \end{bmatrix}; \quad P_2 = \begin{bmatrix} 0.0008 & 0.0004 & 0.0020 \\ 0.0004 & 0.0022 & 0.0123 \\ 0.0020 & 0.0123 & 0.1105 \end{bmatrix} \tag{41}$$

Since $eig(P_1)$ = {0.001, 0.0022, 0.0252} and $eig(P_2)$ = {0.0006, 0.001, 0.1119}, matrices P_1 and P_2 are positive definite and the global asymptotic stability of the PMSM control switched systems is ensured.

The Matlab program shown in Figure 13 is used to calculate the dwell time. A dwell time T = 1.1 ms is obtained.

This is used to demonstrate that in terms of the PMSM control switched systems, system stability is ensured if switching between systems is performed at time intervals at least equal to the dwell time of 1.1 ms.
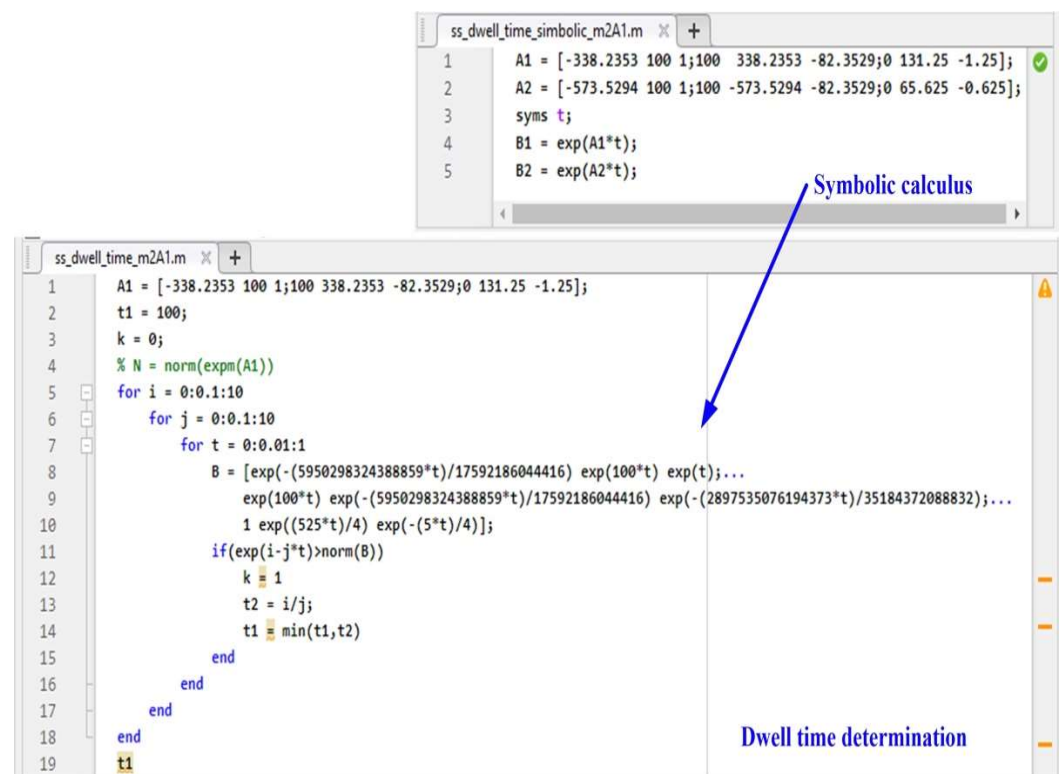

Figure 13. Matlab program for dwell time determination—variable structure 1.

Using Matlab/Simulink, numerical simulations are presented in Figure 14, for the time evolution parameters of the PMSM control switched systems based on FOC-type strategy and switched systems with switching signal type 1, ω_{ref} = [800, 1200] rpm, and T_L = 0.5 Nm.
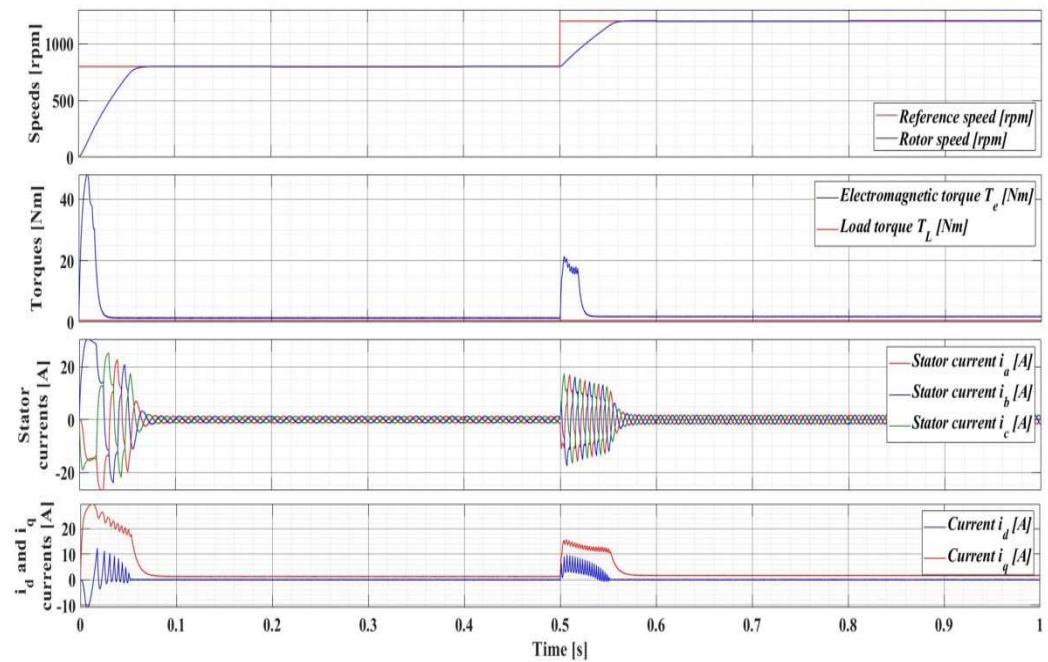
Figure 14. Time evolution parameters for PMSM control system based on FOC-type strategy for PMSM variable structure with switching signal type 1, ω_{ref} = [800, 1200] rpm, and T_L = 0.5 Nm.

Furthermore, Figures 15–17 show the evolution of the states of the PMSM control switched systems (ω, i_q, i_d) in the form of the phase plane for their corresponding combinations. In addition, for two successive PMSM reference speed steps, Figures 18 and 19 show the evolution in the state plane for the PMSM control switched systems. It can be noted that the steady-state conditions are achieved after a relatively fast transient regime and damped oscillations.
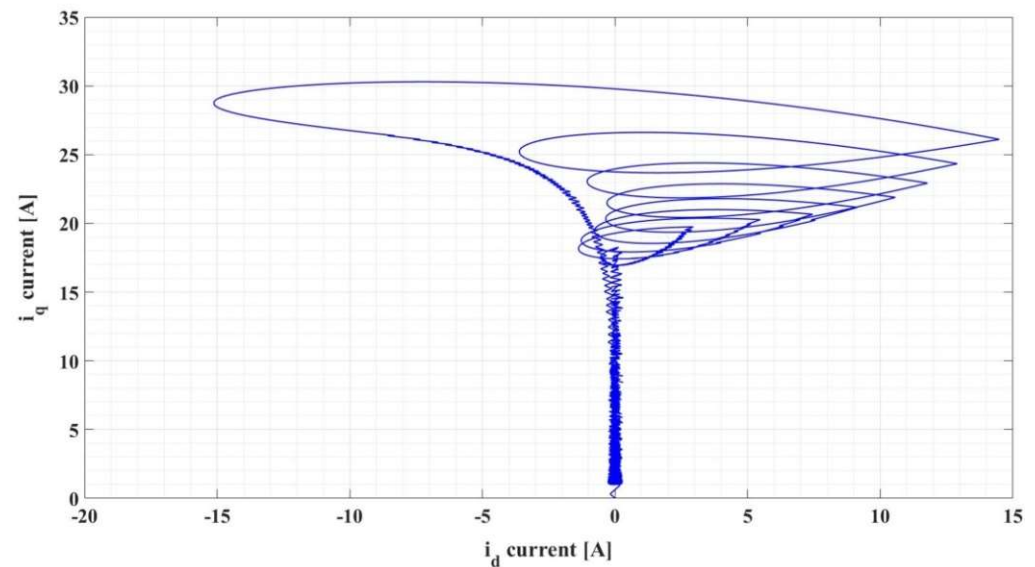

Figure 15. Image of the phase plan for PMSM variable structure with switching signal type 1: i_q current versus i_d current.
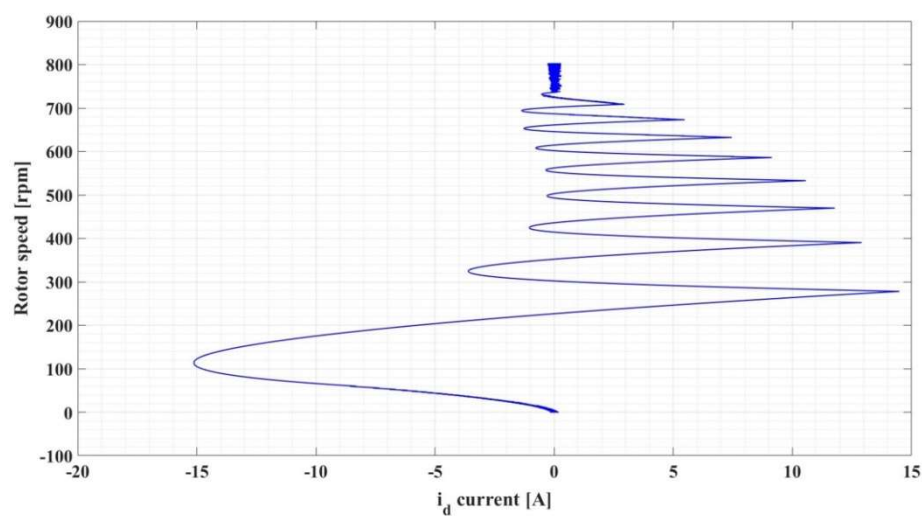
Figure 16. Image of the phase plan for PMSM variable structure with switching signal type 1: rotor speed versus i_d current.
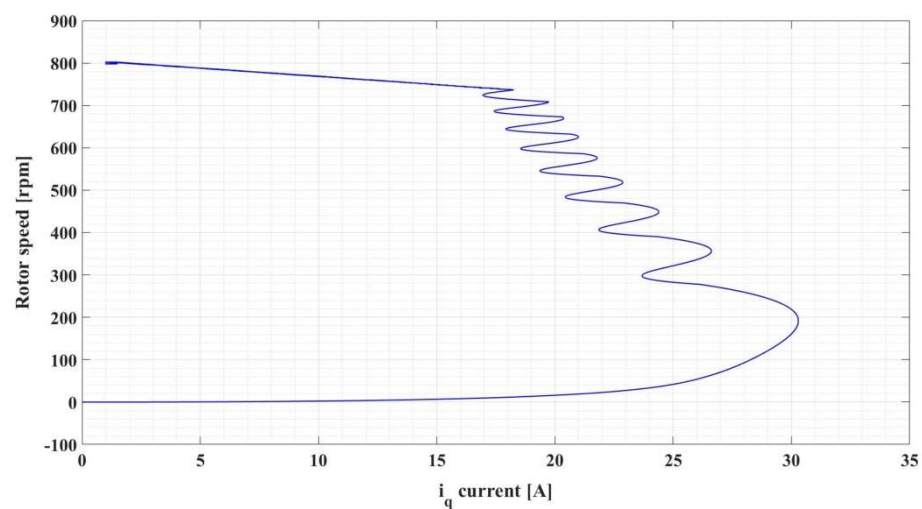

Figure 17. Image of the phase plan for PMSM variable structure with switching signal type 1: rotor speed versus i_q current.
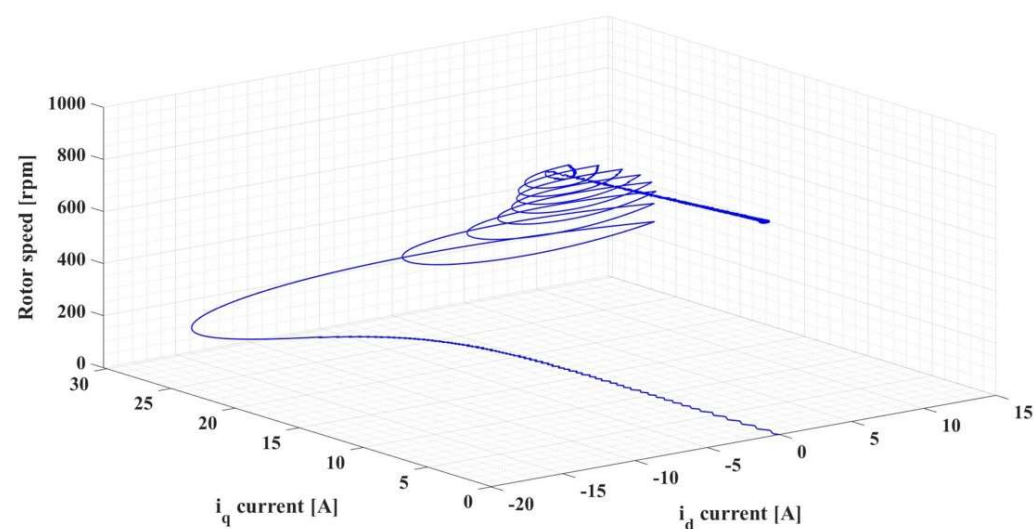

Figure 18. Image of the state space for PMSM variable structure with switching signal type 1: rotor speed versus i_q current versus i_d current (ω_{ref} = 800 rpm).
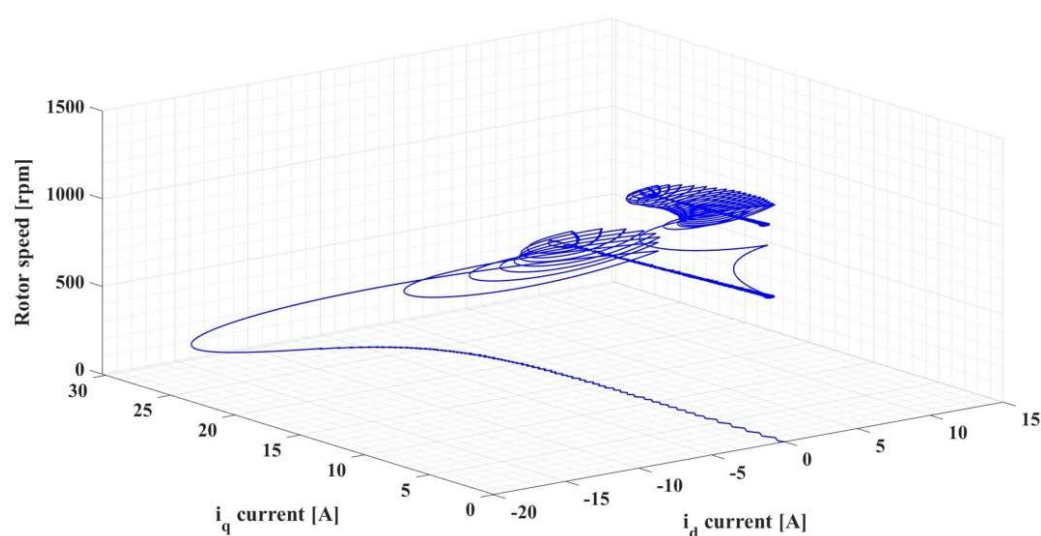
Figure 19. Image of the state space for PMSM variable structure with switching signal type 1: rotor speed versus i_q current versus i_d current (ω_{ref} = [800, 1200] rpm).

Next, it is considered that the variation of the PMSM parameters corresponds to that shown in Table 3.

Table 3. PMSM variation parameters—variable structure 2.

Parameter	Value 1	Value 2	Value 3	Value 4	Unit
R_s	2.875	3.2	4.4	5.6	Ω
L_d and L_q	0.0085	0.01	0.014	0.016	H
J	0.008	0.01	0.014	0.016	kg·m²

Figure 20 presents the Simulink implementation for control switched systems of PMSM based on FOC-type strategy for variable structure with switching signal type 2. The Stateflow Matlab implementation detail for PMSM variable structure used for parameter selection from debug, analysis and time evolution subsystem from Figure 20 is presented in Figure 21.

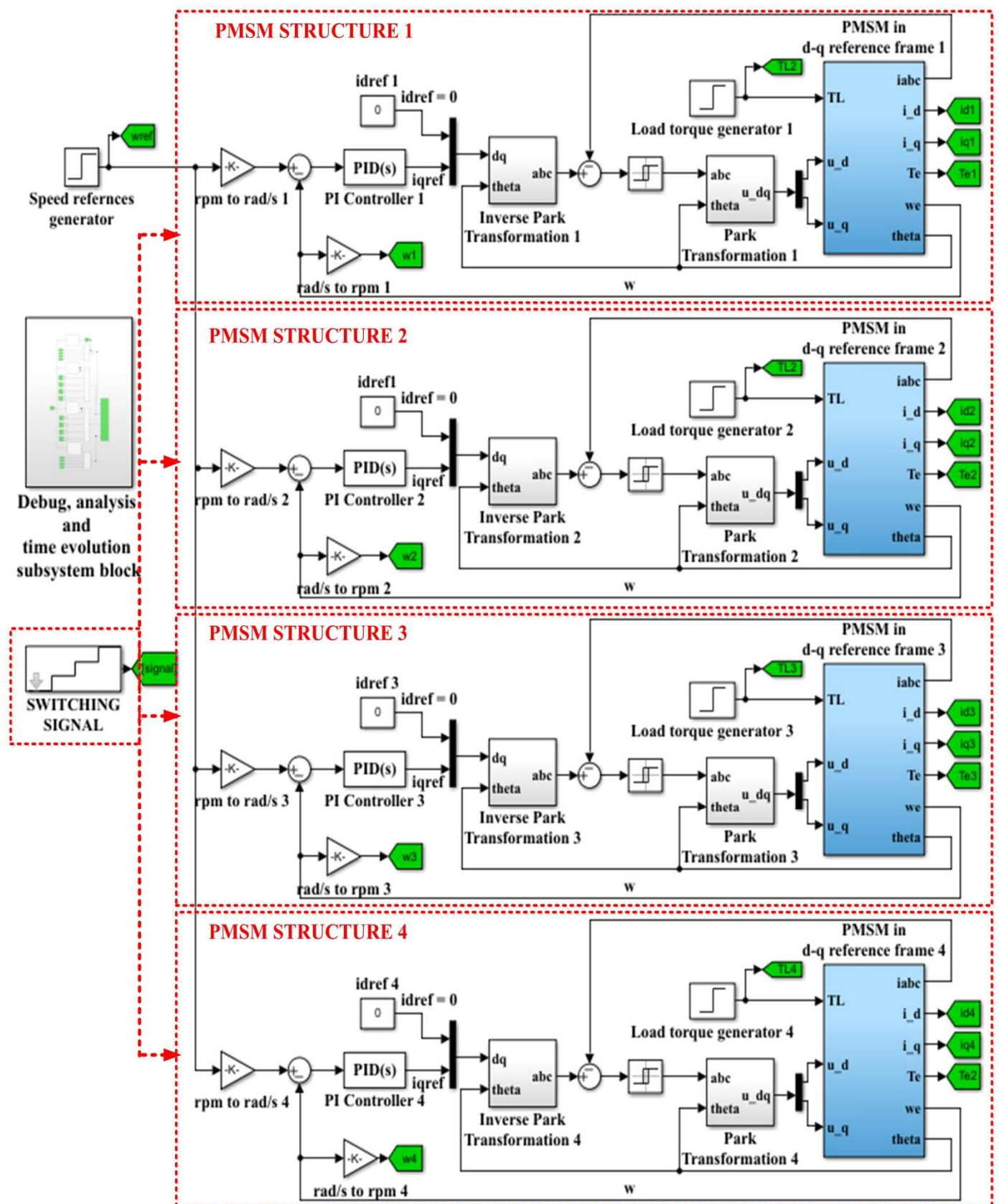The evolution of the switching signal type 2 is presented in Figure 22.

Figure 20. Simulink implementation for PMSM control system based on FOC-type strategy for PMSM variable structure with switching signal type 2.
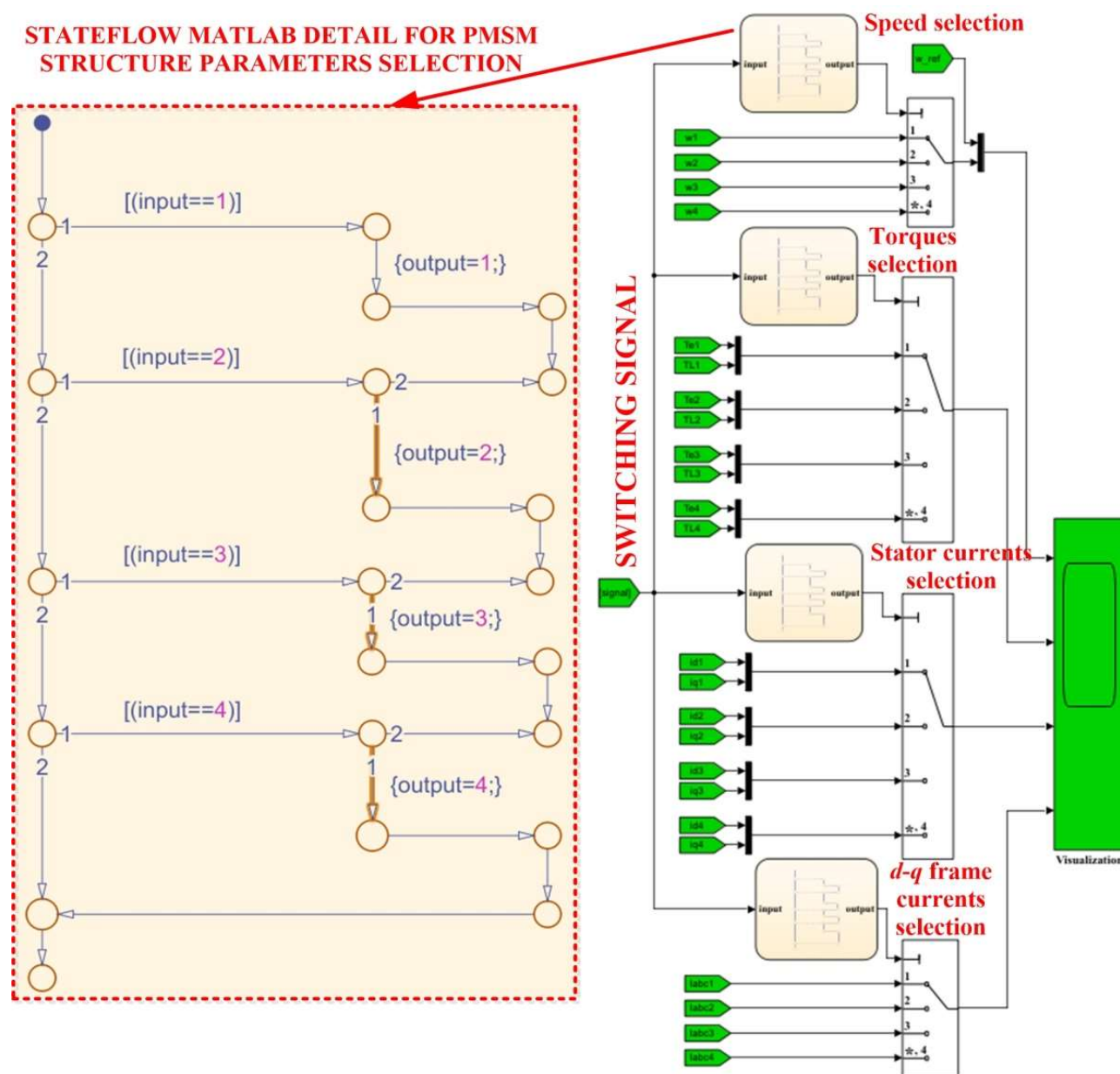
Figure 21. Stateflow Matlab implementation detail for PMSM variable structure used for parameters selection from debug, analysis and time evolution subsystem.
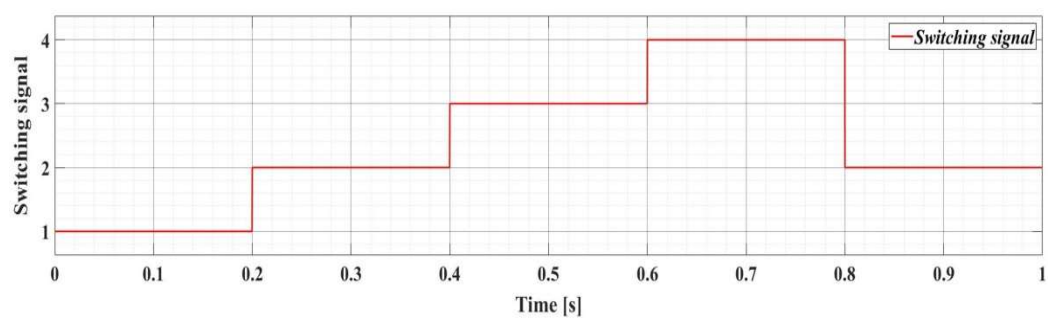

Figure 22. Switching signal type 2.

For the verification of Lyapunov–Metzler inequalities, Figure 23 shows the diagram of a program implemented in Matlab using the YALMIP toolbox.

```
ss_PMSM_m4_calc_soft.m    ×    +
1       addpath(genpath('E:\ARTICOLE 2022\Switched_Systems Automation 2022'))
2       % Parameters
3       R1 = 2.875; R2 = 3.2; R3 = 4.4; R4 = 5.6;
4       L1 = 8.5e-3; L2 = 10e-3; L3 = 14e-3; L4 = 16e-3;
5       J1 = 8e-3; J2 = 10e-3; J3 = 14e-3; J4 = 16e-3;
6       lambda = 0.175; np=4; B = 0.01; Kt = (3/2)*np*lambda;
7       iqref = 2; idref = 0; omegaref = 1000;
8       %Calculate A1, A2, A3, and A4
9       A1 = [-R1/L1 100 1; 100 -R1/L1 -(np*lambda)/L1; 0 Kt/J1 -B/J1]
10      A2 = [-R2/L2 100 1; 100 -R2/L2 -(np*lambda)/L2; 0 Kt/J2 -B/J2]
11      A3 = [-R3/L3 100 1; 100 -R3/L3 -(np*lambda)/L3; 0 Kt/J3 -B/J3]
12      A4 = [-R4/L4 100 1; 100 -R4/L4 -(np*lambda)/L4; 0 Kt/J4 -B/J4]
13      eig(A1); eig(A2); eig(A3); eig(A4);
14      T = 0.0011;
15      % Declare SDP matrices
16      P1 = sdpvar(3,3); P2 = sdpvar(3,3); P3 = sdpvar(3,3); P4 = sdpvar(3,3);
17      % Set LMI
18      T1 = A1'*P1+P1*A1; T2 = A2'*P2+P2*A2; T3 = A3'*P3+P3*A3; T4 = A4'*P4+P4*A4;
19      T5 = expm(A1'*T)*P2*expm(A1*T)-P2;
20      T6 = expm(A1'*T)*P3*expm(A1*T)-P3;
21      T7 = expm(A1'*T)*P4*expm(A1*T)-P4;
22      T8 = expm(A2'*T)*P1*expm(A2*T)-P1;
23      T9 = expm(A2'*T)*P3*expm(A2*T)-P3;
24      T10 = expm(A2'*T)*P4*expm(A2*T)-P4;
25      T11 = expm(A3'*T)*P1*expm(A3*T)-P1;
26      T12 = expm(A3'*T)*P2*expm(A3*T)-P2;
27      T13 = expm(A3'*T)*P4*expm(A3*T)-P4;
28      T14 = expm(A4'*T)*P1*expm(A4*T)-P1;
29      T15 = expm(A4'*T)*P2*expm(A4*T)-P2;
30      T16 = expm(A4'*T)*P3*expm(A4*T)-P3;
31      F = [P1>0; P2>0 ; P3>0; P4>0 ;...
32          T1<0; T2<0; T3<0; T4<0; T5<0; T6<0; T7<0; T8<0;...
33          T9<0; T10<0; T11<0; T12<0; T13<0; T14<0; T15<0; T16<0];
34      about = optimize(F)
35      P1_num = double(P1)
36      P2_num = double(P2)
37      P3_num = double(P3)
38      P4_num = double(P4)
39      eig(P1_num); eig(P2_num); eig(P3_num); eig(P4_num);
```

Figure 23. Matlab program for matrices A_i and P_i determination—case 2.

The matrices A_1, A_2, A_3, and A_4 are given by relations (42) and (43):

$$A_1 = \begin{bmatrix} -338.2353 & 100 & 1 \\ 100 & -338.2353 & -82.3529 \\ 0 & 131.25 & -1.25 \end{bmatrix}; \quad A_2 = \begin{bmatrix} 320 & 100 & 1 \\ 100 & -320 & -70 \\ 0 & 105 & -1 \end{bmatrix} \quad (42)$$

$$A_3 = \begin{bmatrix} -314.2857 & 100 & 1 \\ 100 & -314.2857 & -50 \\ 0 & 75 & -0.7143 \end{bmatrix}; \quad A_4 = \begin{bmatrix} -350 & 100 & 1 \\ 100 & -350 & -43.75 \\ 0 & 65.625 & -0.625 \end{bmatrix} \quad (43)$$

Using the Matlab environment, the eigenvalues are calculated as follows: $eig(A_1) = \{-426.1689, -209.2358, -42.316\}$, $eig(A_2) = \{-411.3163, -200.1138, -29.5699\}$, $eig(A_3) = \{-409.7148, -204.8635, -14.7075\}$, and $eig(A_4) = \{-446.7605, -244.064, -9.8005\}$. As a result, A_1, A_2, A_3, and A_4 are Hurwitz matrices.

Using the Matlab environment and YALMIP toolbox, the matrices P_1, P_2, P_3, and P_4 containing the solution to the system are obtained as follows:

$$P_1 = \begin{bmatrix} 0.051 & 0.0367 & 0.0458 \\ 0.0367 & 0.1209 & 0.188 \\ 0.0458 & 0.188 & 0.6182 \end{bmatrix}; \quad P_2 = \begin{bmatrix} 0.0573 & 0.0395 & 0.0496 \\ 0.0395 & 0.1189 & 0.193 \\ 0.0496 & 0.193 & 0.6897 \end{bmatrix} \tag{44}$$

$$P_3 = \begin{bmatrix} 0.0589 & 0.0379 & 0.0459 \\ 0.0379 & 0.1036 & 0.155 \\ 0.0459 & 0.155 & 0.5965 \end{bmatrix}; \quad P_4 = \begin{bmatrix} 0.0462 & 0.0271 & 0.0287 \\ 0.0271 & 0.0769 & 0.0986 \\ 0.0287 & 0.0986 & 0.4136 \end{bmatrix} \tag{45}$$

Since $eig(P_1) = \{0.0311, 0.0730, 0.6860\}$, $eig(P_2) = \{0.0326, 0.0795, 0.7539\}$, $eig(P_3) = \{0.0326, 0.0801, 0.6463\}$, and $eig(P_4) = \{0.0278, 0.0656, 0.4434\}$, matrices P_i are positive definite and the global asymptotic stability of the PMSM control switched systems is ensured.

Moreover, for this variable structure with switching signal 2, the Matlab program shown in Figure 24 is also used to calculate the dwell time.

The dwell time $T = 1.1$ ms. This have been used to demonstrate that, in terms of the PMSM control switched systems (variable structure type 2), system stability is ensured if switching between systems is performed at time intervals at least equal to the dwell time of 1.1 ms.

```
ss_dwell_time_simbolic_m4A.m    +
1    A1 = [-338.2353 100 1;100 -338.2353 -82.3529;0 131.25 -1.25];
2    A2 = [-320 100 1;100 -320 -70;0 105 -1];
3    A3 = [-314.2857 100 1;100 -314.2857 -50;0 75 -0.7143];
4    A4 = [-350 100 1;100 -350 -43.75;0 65.625 -0.625];
5    syms t;
6    B1 = exp(A1*t);
7    B2 = exp(A2*t);
8    B3 = exp(A3*t);
9    B4 = exp(A4*t);
```
Symbolic calculus

```
ss_dwell_time_m4A44.m    +
1    A4 = [-350 100 1;100 -350 -43.75;0 65.625 -0.625];
2    t1 = 100;
3    k = 0;
4    % N = norm(expm(A1))
5    for i = 0:0.1:100
6        for j = 0:0.1:100
7            for t = 0:0.01:1
8                B = [exp(-350*t) exp(100*t) exp(t);...
9                     exp(100*t) exp(-350*t) exp(-(175*t)/4);...
10                    1 exp((525*t)/8) exp(-(5*t)/8)];
11               if(exp(i-j*t)>norm(B))
12                   k = 1
13                   t2 = i/j;
14                   t1 = min(t1,t2)
15               end
16           end
17       end
18   end
19   t1
```
Dwell time determination

Figure 24. Matlab program for dwell time determination—variable structure 2.

The time evolution for PMSM control system based on FOC-type strategy for PMSM variable structure with switching signal type 2, ω_{ref} = [800, 1200] rpm, and T_L = 0.5 Nm is presented in Figure 25.
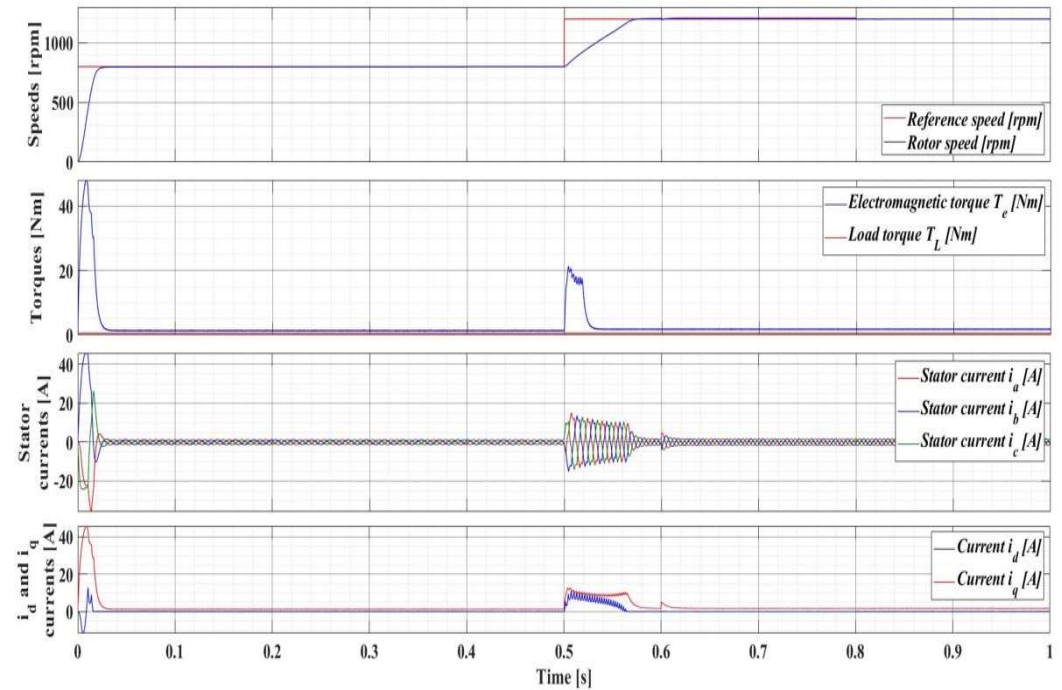

Figure 25. Time evolution for PMSM control system based on FOC-type strategy for PMSM with variable structure and switching signal type 2, ω_{ref} = [800 1200] rpm, and T_L = 0.5 Nm.

Figures 26, 27, 28, 29, 30 and 31 show the evolution of the states of the PMSM control switched systems with variable structure and switching signal type 2 (ω, i_q, i_d) in the form of the phase plane for ω_{ref} = 800 rpm and ω_{ref} = [800, 1200] rpm, respectively.

For two successive reference speed steps of PMSM ω_{ref} = [800, 1200] rpm, Figures 32 and 33 show the evolution in the state plane for the PMSM control switched systems with variable structure and switching signal type 2.

It can be noted that the steady-state conditions are achieved after a relatively fast transient regime and damped oscillations.
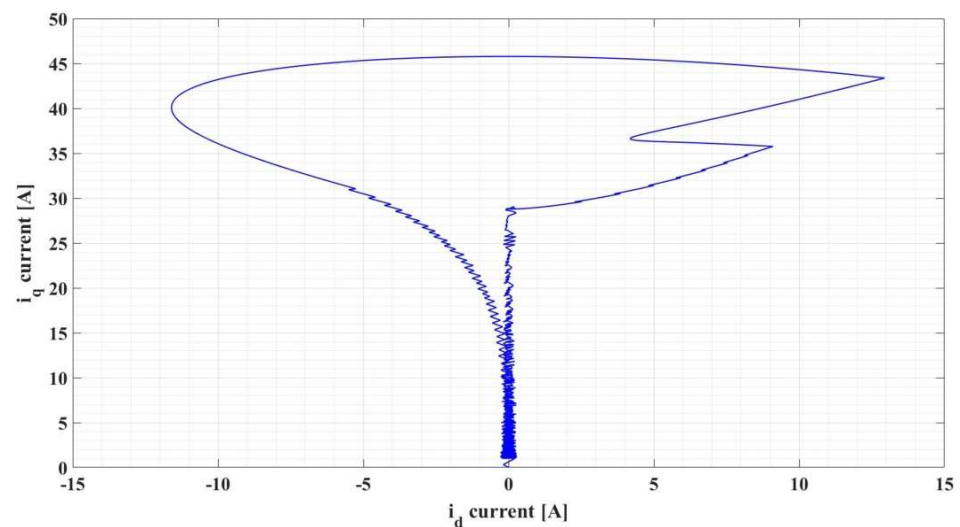

Figure 26. Image of the phase plan for PMSM variable structure with switching signal type 2: i_q current versus i_d current (ω_{ref} = 800 rpm).
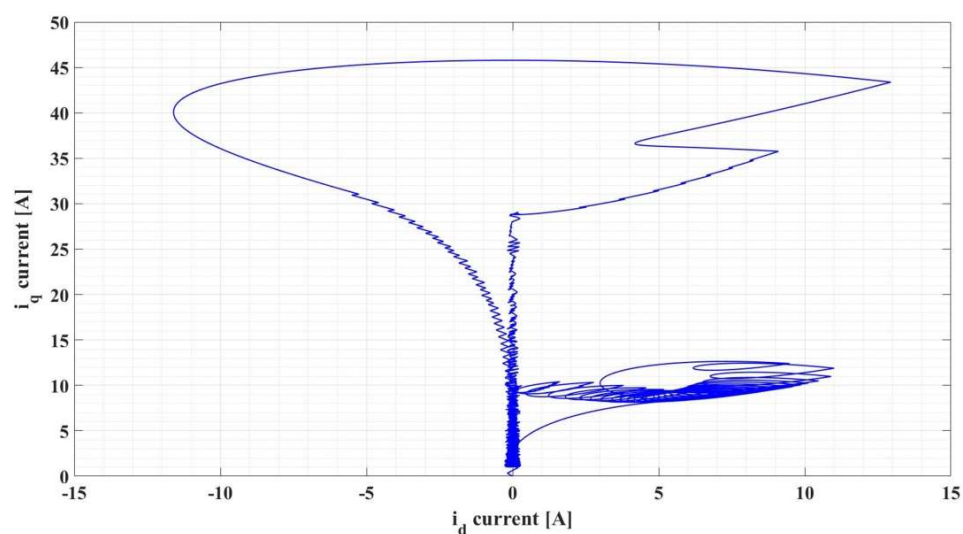
Figure 27. Image of the phase plan for PMSM variable structure with switching signal type 2: i_q current versus i_d current (ω_{ref} = [800, 1200] rpm).
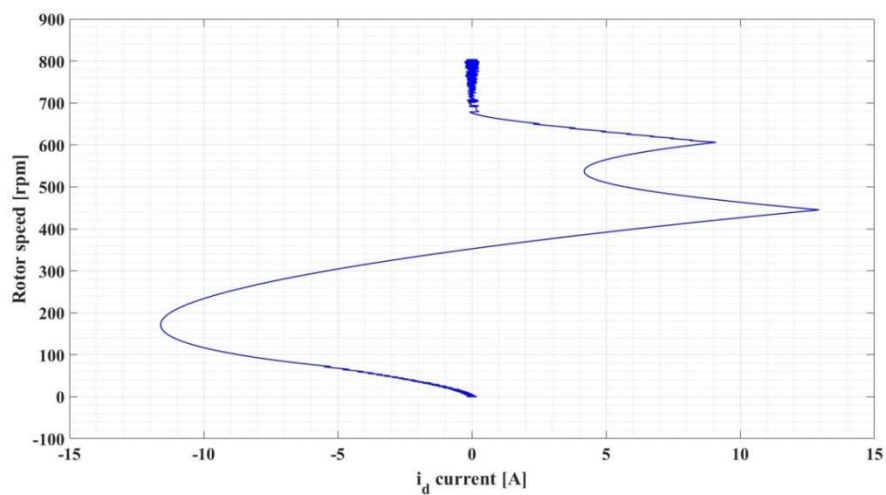

Figure 28. Image of the phase plan for PMSM variable structure with switching signal type 2: rotor speed versus i_d current (ω_{ref} = 800 rpm).

Figure 29. Image of the phase plan for PMSM variable structure with switching signal type 2: rotor speed versus i_d current (ω_{ref} = [800, 1200] rpm).

Figure 30. Image of the phase plan for PMSM variable structure with switching signal type 2: rotor speed versus i_q current (ω_{ref} = 800 rpm).
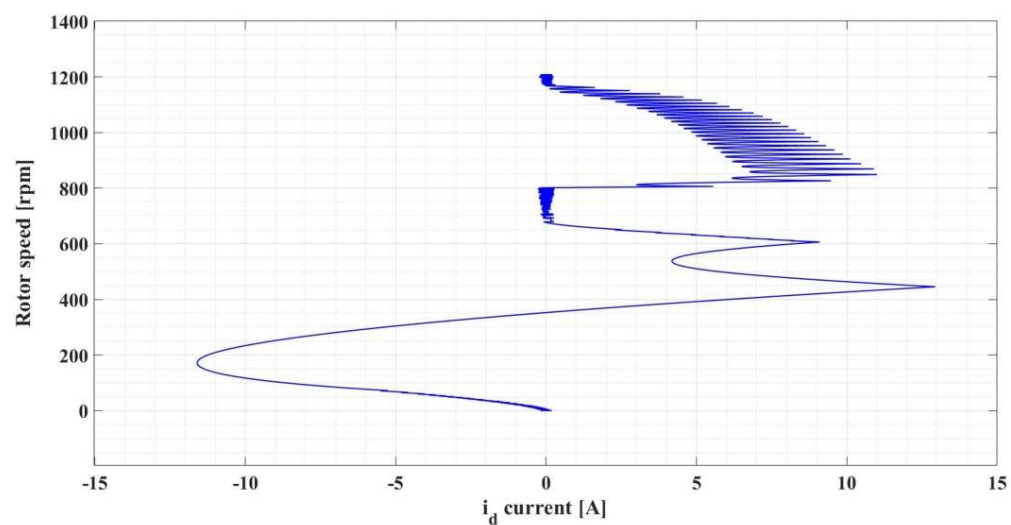

Figure 31. Image of the phase plan for PMSM variable structure with switching signal type 2: rotor speed versus i_q current (ω_{ref} = [800, 1200] rpm).
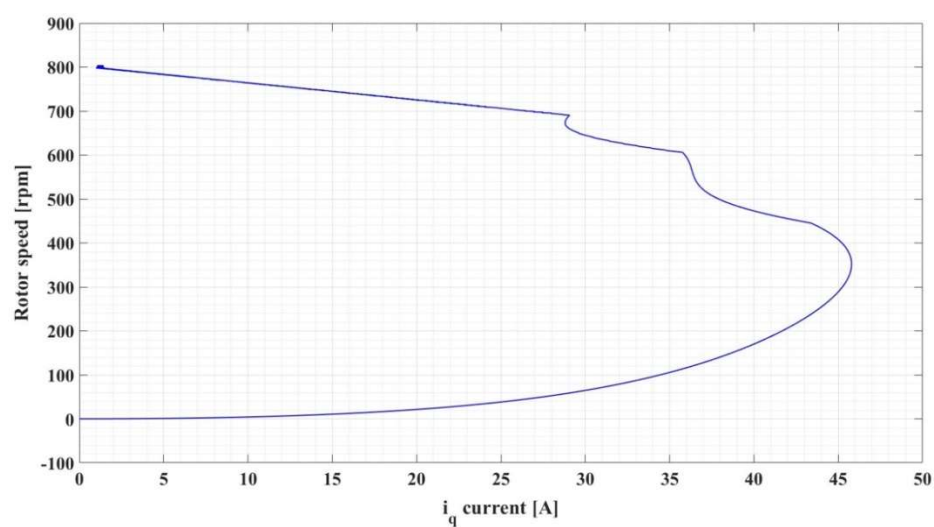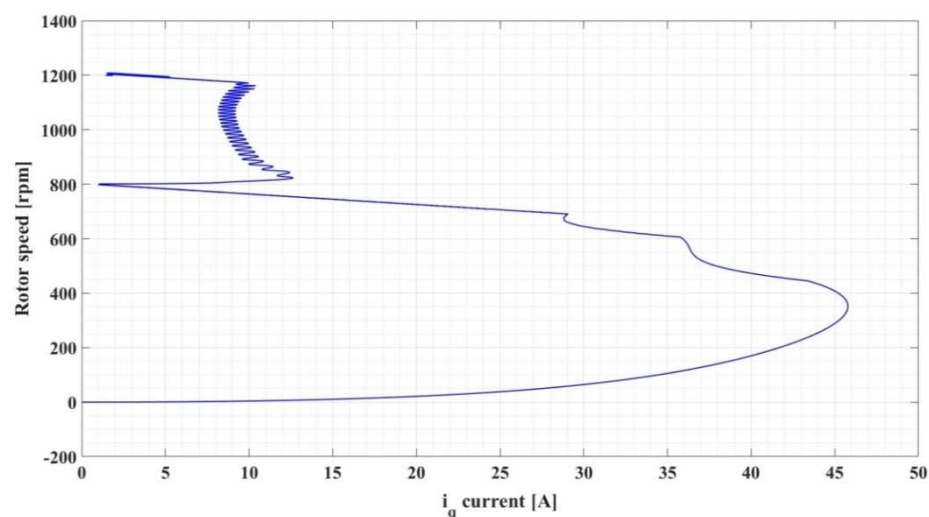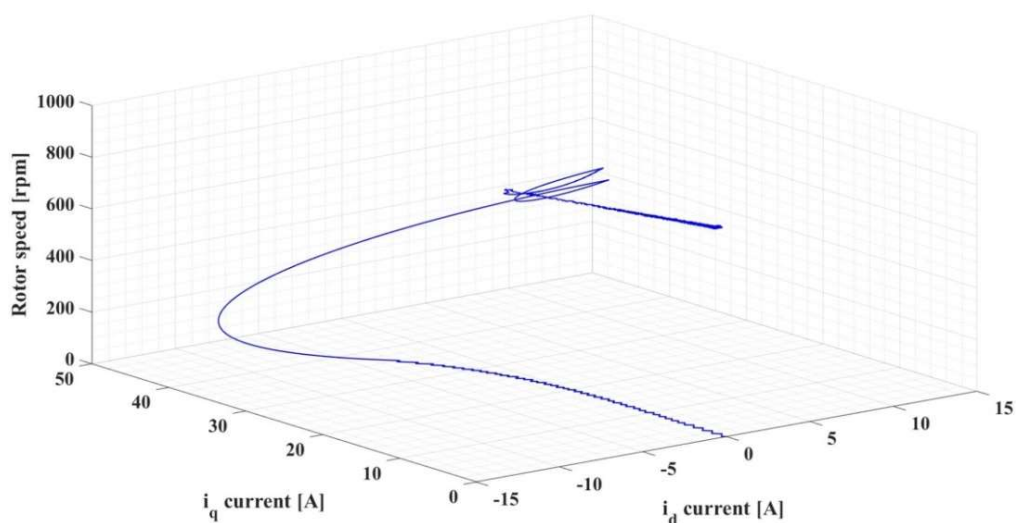

Figure 32. Image of the state space for PMSM variable structure with switching signal type 2: rotor speed versus i_q current versus i_d current (ω_{ref} = 800 rpm).
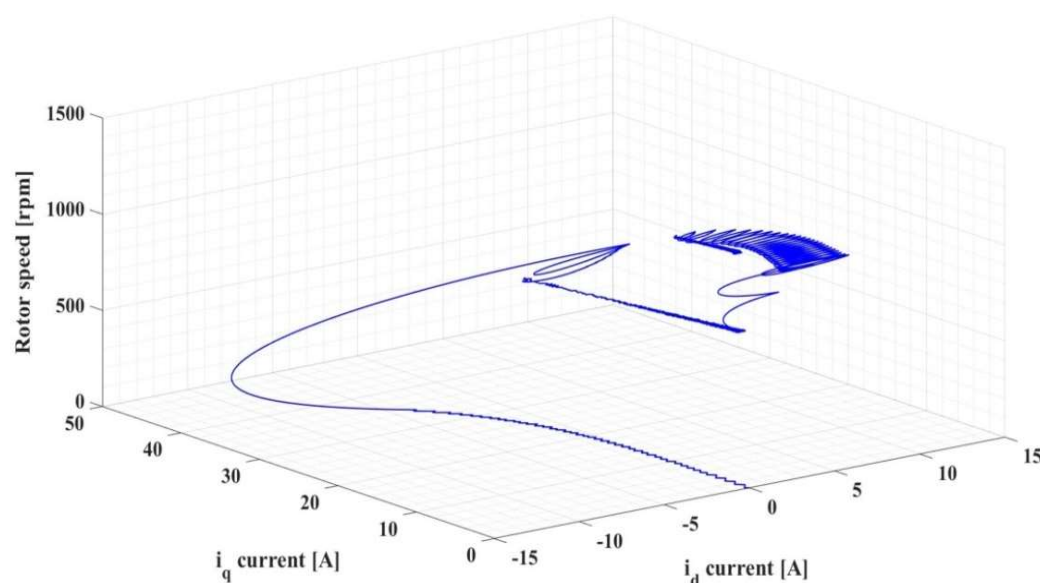
Figure 33. Image of the state space for PMSM variable structure with switching signal type 2: rotor speed versus i_q current versus i_d current (ω_{ref} = [800, 1200] rpm).

Moreover, as in the case of variable structure and switching signal type 1, compared to the evolution of the states for the PMSM control system where the parameters remain constant (case presented at the beginning of Section 4), slight additional oscillations are noted due to the switching between the various parametric structures of the PMSM, preserving stability and overall performance without affecting the qualitative picture of the evolution of the system given by the state space.

In synthesis in this section, three examples are considered: the model of a PMSM controlled with FOC, the model of a PMSM in which the parametric variations contribute to the definition of two PMSM models, and the model of a PMSM in which the parametric variations contribute to the definition of four PMSM models. After calculating the dwell time and checking the Lyapunov–Metzler inequalities, the conclusion of PMSM stability can be drawn using switched systems theory. On the other hand, just to confirm the results obtained using the FOC strategy, the state space portraits are presented for the qualitative analysis of the system's behavior, confirming the stability and parametric robustness of the system.

According to Example 2 in Section 3, it is proven once again that local stability does not imply global stability, in the sense that although each subsystem is stable, the evolution of the entire switched systems can be unstable. This means that although using the classic methods of stability analysis mentioned above, each subsystem is stable, but the mode of transition between these systems is not taken into consideration, thus implying that the switched systems could be unstable. This discrepancy in the analysis of the stability of the switched systems is resolved by specific means, namely by introducing the notion of dwell time and solving the Lyapunov–Metzler type inequalities.

It can be concluded that, by using the switched systems theory in the presented example of PMSM control, the FOC control strategy is a control strategy that ensures parametric robustness, in the sense that in case of significant variations of the parameters in the PMSM structure, the overall performance of the control system is preserved both qualitatively and quantitatively.

5. Conclusions

Usually, the parameters of a PMSM vary over time, and the study of the parametric robustness of the PMSM control systems becomes an important step in the chain of control system design. Using switched-systems theory, elements have been presented regarding

the demonstration of the stability of switched systems by solving Lyapunov–Metzler inequalities, where the switching signal frequency is lower than the switching frequency given by the dwell time. An algorithm for calculating the dwell time has also been defined and presented. Numerical simulations performed in Simulink validate the fact that, for parametric variations of the PMSM structure, the PMSM control switched systems preserve the qualitative performance in terms of its control. A series of Matlab programs based on the YALMIP toolbox for obtaining *Pi* matrices and dwell time are presented to demonstrate the stability and performance of the PMSM control switched systems. In this paper, the stability demonstration was achieved using elements of the switched systems theory, while the PMSM control structure was a predefined FOC structure. In future papers, we will propose the implementation of control laws whose synthesis is derived from specific elements of the switched-systems theory. Moreover, one of our directions of research will involve the study of approximate controllability of fractional integrodifferential equations using resolvent operators [35].

Author Contributions: Conceptualization, M.N.; data curation, M.N. and D.S.; formal analysis, M.N., C.-I.N., D.S. and C.I.; funding acquisition, M.N.; investigation, M.N., C.-I.N. and D.S.; methodology, M.N., C.-I.N., D.S. and C.I.; project administration, M.N.; resources, M.N., C.-I.N. and D.S.; software, M.N. and C.-I.N.; supervision, M.N., D.S. and C.I.; validation, M.N. and C.-I.N.; visualization, M.N., C.-I.N., D.S. and C.I.; writing—original draft, M.N. and C.-I.N.; writing—review and editing, M.N. and C.-I.N. All authors have read and agreed to the published version of the manuscript.

Institutional Review Board Statement: Not applicable.

Informed Consent Statement: Not applicable.

Data Availability Statement: Not applicable.

Conflicts of Interest: The authors declare no conflict of interest.

Nomenclature

PMSM	Permanent Magnet Synchronous Motor
FOC	Field Oriented Control
DTC	Direct Torque Control
YALMIP	A toolbox for modeling and optimization in MATLAB
R_s	Stator resistance of the PMSM
R_d and R_q	Stator resistances on *d-q* axis
L_d and L_q	Stator inductances on *d-q* axis
u_d and u_q	Stator voltages on *d-q* axis
i_d and i_q	Stator currents on *d-q* axis
T_L	Load torque
J	Combined inertia of PMSM rotor and load
B	Combined viscous friction of PMSM rotor and load
λ_0	Flux induced by the permanent magnets of the rotor in the stator phases
n_p	Pole pairs number
ω	PMSM rotor speed

References

1. Wang, S.-C.; Nien, Y.-C.; Huang, S.-M. Multi-Objective Optimization Design and Analysis of V-Shape Permanent Magnet Synchronous Motor. *Energies* **2022**, *15*, 3496.
2. You, Y.-M. Optimal Design of PMSM Based on Automated Finite Element Analysis and Metamodeling. *Energies* **2019**, *12*, 4673.
3. Furmanik, M.; Gorel, L.; Konvičný, D.; Rafajdus, P. Comparative Study and Overview of Field-Oriented Control Techniques for Six-Phase PMSMs. *Appl. Sci.* **2021**, *11*, 7841.
4. Feng, S.; Jiang, W.; Zhang, Z.; Zhang, J.; Zhang, Z. Study of efficiency characteristics of Interior Permanent Magnet Synchronous Motors. *IEEE Trans. Magn.* **2018**, *54*, 8108005.

5. Zakharov, V.; Minav, T. Analysis of Field Oriented Control of Permanent Magnet Synchronous Motor for a Valveless Pump-Controlled Actuator. *Multidiscip. Digit. Publ. Inst. Proc.* **2020**, *64*, 19.

6. Jiang, W.; Han, W.; Wang, L.; Liu, Z.; Du, W. Linear Golden Section Speed Adaptive Control of Permanent Magnet Synchronous Motor Based on Model Design. *Processes* **2022**, *10*, 1010.

7. Wang, D.; Yuan, T.; Wang, X.; Wang, X.; Wang, S.; Ni, Y. Performance Improvement for PMSM Driven by DTC Based on Discrete Duty Ratio Determination Method. *Appl. Sci.* **2019**, *9*, 2924.

8. Amin, F.; Sulaiman, E.B.; Utomo, W.M.; Soomro, H.A.; Jenal, M.; Kumar, R. Modelling and Simulation of Field Oriented Control based Permanent Magnet Synchronous Motor Drive System. *Indones. J. Electr. Eng. Comput. Sci.* **2017**, *6*, 387.

9. Qiu, H.; Zhang, H.; Min, L.; Ma, T.; Zhang, Z. Adaptive Control Method of Sensorless Permanent Magnet Synchronous Motor Based on Super-Twisting Sliding Mode Algorithm. *Electronics* **2022**, *11*, 3046.

10. Chen, H.; Yao, Z.; Liu, Y.; Lin, J.; Wang, P.; Gao, J.; Zhu, S.; Zhou, R. PMSM Adaptive Sliding Mode Controller Based on Improved Linear Dead Time Compensation. *Actuators* **2022**, *11*, 267.

11. Tang, M.; Zhuang, S. On Speed Control of a Permanent Magnet Synchronous Motor with Current Predictive Compensation. *Energies* **2019**, *12*, 65.

12. Nicola, M.; Nicola, C.-I. Sensorless Predictive Control for PMSM Using MRAS Observer. In Proceedings of the International Conference on Electromechanical and Energy Systems (SIELMEN), Craiova, Romania, 9–11 October 2019; pp. 1–7.

13. Mayilsamy, G.; Natesan, B.; Joo, Y.H.; Lee, S.R. Fast Terminal Synergetic Control of PMVG-Based Wind Energy Conversion System for Enhancing the Power Extraction Efficiency. *Energies* **2022**, *15*, 2774.

14. Nicola, M.; Nicola, C.-I. Sensorless Fractional Order Control of PMSM Based on Synergetic and Sliding Mode Controllers. *Electronics* **2020**, *9*, 1494.

15. Nicola, M.; Duta, M.; Nitu, M.; Aciu, A.; Nicola, C.-I. Improved System Based on ANFIS for Determining the Degree of Polymerization. *Adv. Sci. Technol. Eng. Syst. J.* **2022**, *5*, 664–675.

16. Hoai, H.-K.; Chen, S.-C.; Chang, C.-F. Realization of the Neural Fuzzy Controller for the Sensorless PMSM Drive Control System. *Electronics* **2020**, *9*, 1371.

17. Nicola, M.; Nicola, C.-I. Tuning of PI Speed Controller for PMSM Control System Using Computational Intelligence. In Proceedings of the 21st International Symposium on Power Electronics (Ee), Novi Sad, Serbia, 27–30 October 2021; pp. 1–6.

18. Nicola, M.; Nicola, C.-I.; Selișteanu, D. Improvement of PMSM Sensorless Control Based on Synergetic and Sliding Mode Controllers Using a Reinforcement Learning Deep Deterministic Policy Gradient Agent. *Energies* **2022**, *15*, 2208.

19. Ullah, K.; Guzinski, J.; Mirza, A.F. Critical Review on Robust Speed Control Techniques for Permanent Magnet Synchronous Motor (PMSM) Speed Regulation. *Energies* **2022**, *15*, 1235.

20. Zhang, Q.; Yu, R.; Li, C.; Chen, Y.-H.; Gu, J. Servo Robust Control of Uncertain Mechanical Systems: Application in a Compressor/PMSM System. *Actuators* **2022**, *11*, 42.

21. Ma, Y.; Li, Y. Active Disturbance Compensation Based Robust Control for Speed Regulation System of Permanent Magnet Synchronous Motor. *Appl. Sci.* **2020**, *10*, 709.

22. Liu, C.; Liu, X. Stability of Switched Systems with Time-Varying Delays under State-Dependent Switching. *Mathematics* **2022**, *10*, 2722.

23. Halanay, A.; Samuel, J. *Differential Equations, Discrete Systems and Control: Economic Models (Mathematical Modelling: Theory and Applications*; Kluwer Academic Publishers: Dordrecht, The Netherlands, 1997; pp. 15–123.

24. Colaneri, P. *Analysis and Control of Linear Switched Systems*; The Polytechnic University of Milano: Milan, Italy, 2009. Available online: https://colaneri.faculty.polimi.it/Lucidi-Bertinoro-2009.pdf (accessed on 15 February 2022).

25. Ren, W.; Xiong, J. Robust Filtering for 2-D Discrete-Time Switched Systems. *IEEE Trans. Autom. Control* **2021**, *66*, 4747–4760.

26. Ligang, W.; Rongni, Y.; Peng, S.; Xiaojie, S. Stability analysis and stabilization of 2-D switched systems under arbitrary and restricted switchings. *Automatica* **2015**, *59*, 206–215.

27. Meng, F.; Shen, X.; Li, X. Stability Analysis and Synthesis for 2-D Switched Systems with Random Disturbance. *Mathematics* **2022**, *10*, 810.

28. Krok, M.; Hunek, W.P.; Feliks, T. Switching Perfect Control Algorithm. *Symmetry* **2020**, *12*, 816.

29. Nicola, C.-I.; Nicola, M. Real Time Implementation of the PMSM Sensorless Control Based on FOC Strategy. In Proceedings of the 4th Global Power, Energy and Communication Conference (GPECOM), Nevsehir, Turkey, 14–17 June 2022; pp. 179–183.

30. Löfberg, J. Automatic robust convex programming. *Optim. Methods Softw.* **2022**, *27*, 115–129.

31. Besselmann, T.; Lofberg, J.; Morari, M. Explicit MPC for LPV Systems: Stability and Optimality. *IEEE Trans. Autom. Control* **2012**, *57*, 2322–2332.

32. Chandrasekaran, V.; Shah, P. Relative entropy optimization and its applications. *Math. Program. Ser. A* **2016**, *161*, 1–32.

33. Löfberg, J. YALMIP : A Toolbox for Modeling and Optimization in MATLAB. In Proceedings of the IEEE International Conference on Robotics and Automation (IEEE Cat. No.04CH37508), Taipei, Taiwan, 2–4 September 2004, pp. 284–289.

34. Nicola, M.; Nicola, C.-I.; Ionete, C.; Șendrescu, D.; Roman, M. Improved Performance for PMSM Control Based on Robust Controller and Reinforcement Learning. In Proceedings of the 26th International Conference on System Theory, Control and Computing (ICSTCC), Sinaia, Romania, 19–21 October 2022; pp. 207–212.

35. Vijayakumar, V.; Nisar, K.S.; Chalishajar, D.; Shukla, A.; Malik, M.; Alsaadi, A.; Aldosary, S.F. A Note on Approximate Controllability of Fractional Semilinear Integrodifferential Control Systems via Resolvent Operators. *Fractal Fract.* **2022**, *6*, 73.